ACCESS

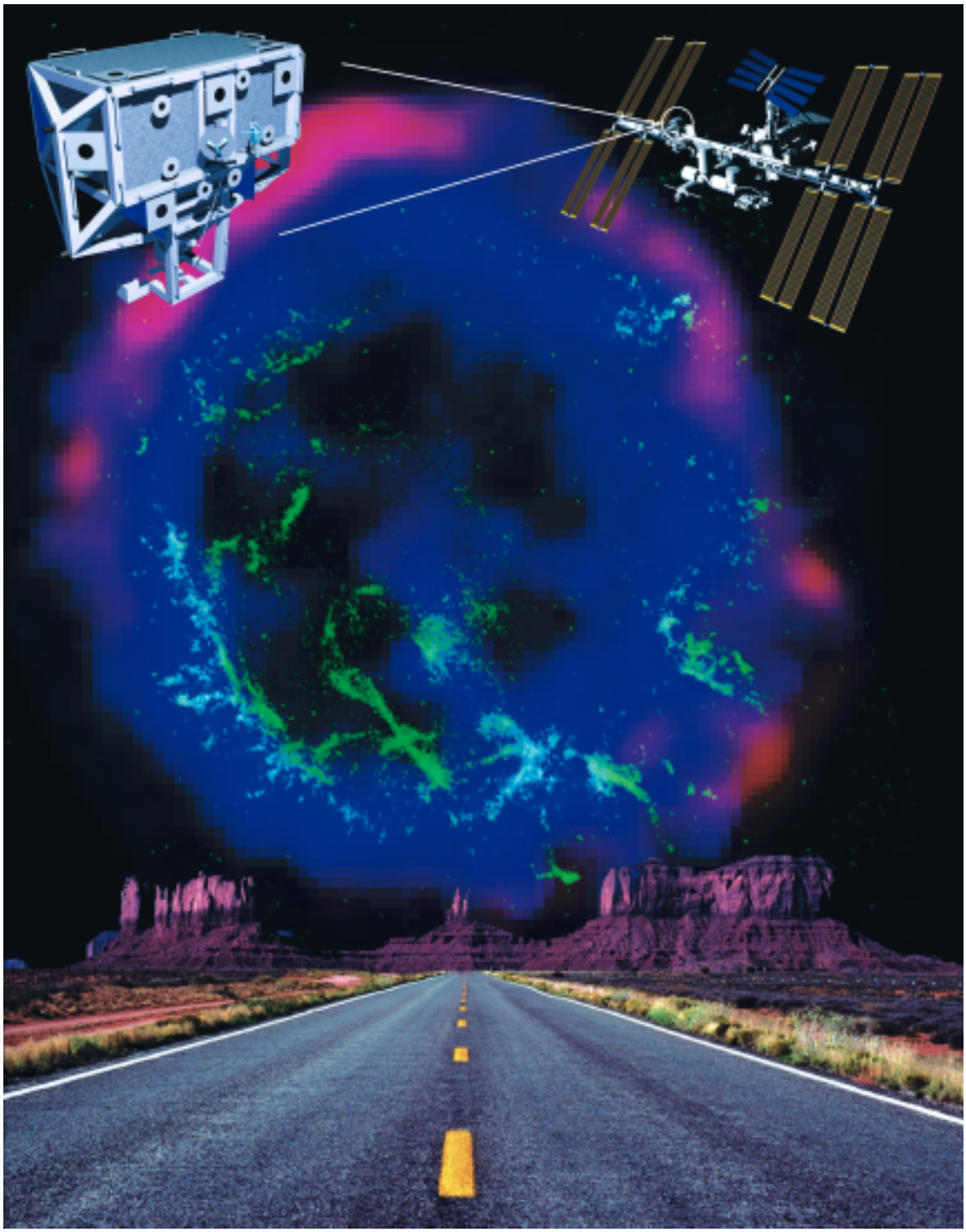

A Cosmic Journey

ACCESS

Advanced **C**osmic-ray **C**omposition **E**xperiment
for the **S**pace **S**tation

ACCESS:
A Cosmic Journey

Formulation Study Report of the ACCESS Working Group

Report published at the NASA Goddard Space Flight Center

November 2000

Cover image: ACCESS mounted on the Space Station. Supernovae are the source most frequently suggested to provide the energy powering the cosmic radiation. Supernova remnant E0102-72 is shown here in a color composite image of X-rays (blue), radio (red) and optical (green). This supernova exploded around 190,000 years ago in the Small Magellanic Cloud.

The ACCESS Team

The ACCESS Working Group (AWG) included a broad spectrum of interested members of the cosmic-ray community. Key groups within the AWG include:

ACCESS Investigator Working Group (IWG)
Robert E. Streitmatter, NASA GSFC (Co-Chair, Study Scientist)
Simon P. Swordy, University of Chicago (Co-Chair)
W. Robert Binns, Washington University
Michael L. Cherry, Louisiana State University
Stephane Coutu, Pennsylvania State University
Richard A. Mewaldt, California Institute of Technology
Dietrich Müller, University of Chicago
Jonathan F. Ormes, NASA GSFC
Thomas A. Parnell, NASA MSFC
Eun-Suk Seo, University of Maryland
Steven J. Stochaj, New Mexico State University
Gregory Tarlé, University of Michigan
John P. Wefel, Louisiana State University
Richard Wigmans, Texas Tech University

ACCESS Executive Committee
Martin H. Israel, Washington University, St. Louis (Chair)
Thomas K. Gaisser, University of Delaware (former member)
Frank C. Jones, NASA GSFC
Frank B. McDonald, University of Maryland
Robert E. Streitmatter, NASA GSFC (Study Scientist, AWG Co-Chair)
Simon P. Swordy, University of Chicago (AWG Co-Chair)
Gaurang B. Yodh, University of California, Irvine

ACCESS Study Team Leaders
Rudy Larsen, NASA GSFC (Formulation Manager)
Elizabeth A. Park, NASA GSFC (previous Formulation Manager)
Thomas K. Gaisser, University of Delaware (previous Theory Team Chair)
Frank C. Jones, NASA GSFC (Theory Team Chair)
John W. Mitchell, NASA GSFC (Accelerator Test Team Coordinator)
Jonathan F. Ormes, NASA GSFC (Simulation Team Chair)

Other AWG participants included: James Adams (NASA MSFC), Louis Barbier (NASA GSFC), James Beatty (Penn State), Ulisse Bravar (NMSU), Gary Case (LSU), Eric Christian (NASA GSFC), Mark Christl (NASA MSFC), Donald Ellison (NC State), Opher Ganel (U Md), Gregory Guzik (LSU), Paul Hink (Wash U), Leonard Howell (NASA MSFC), Joachim Isbert (LSU), Hong Joo Kim (Seoul National U), Son Kee Kim (Seoul National U), Jeongin Lee (NASA MSFC), Shawn McKee (U Mich), Alex Moiseev (NASA GSFC), James Musser (Indiana U), Vladimir Nagasalev (Texas Tech), Lawrence Pinsky (U Houston), Carlos Salgado (Norfolk State U), Alan Sill (Texas Tech), Manfred Simon (U Siegen), Ramin Sina (U Md), Yoshi Takahashi (U Alabama), Andrea Vacchi (U Trieste), Jian-Zhong Wang (U Md), John Watts (NASA MSFC), Andrew Westphal (UC Berkeley), Mark Wiedenbeck (NASA JPL), and Thomas Wilson (NASA JSC).

This report was assembled under the direction of the Editorial Committee: Martin Israel, Frank Jones, Rudy Larsen, Robert Streitmatter, and Simon Swordy. The report includes essential contributions from Louis Barbier and Eric Christian (Deputy Study Scientists), Stephane Coutu, Donald Ellison, Dietrich Müller, Gregory Tarlé, John Wefel, and Gaurang Yodh. The committee acknowledges valuable advice and constant encouragement from Vernon Jones and James Ling of NASA Headquarters. The committee is particularly grateful to Beth Jacob for extensive technical assistance and perceptive editorial advice. Technical work for this report was ably supplied by the NASA GSFC Engineering Study Team: Rudy Larsen, Elizabeth Park, Howard Branch, Jason Budinoff, Ruth Carter, Christine Collins, Roger Counts, John Crow, Bob Eby, Tom Flatley, Ludie Kidd, Charles Kim, Dolf Lekebusch, Ruthan Lewis, John Lindsay, David Robinson, Rebecca Roller, Steve Tompkin, and Diane Yun.

Table of Contents

Executive Summary 4
1. Introduction 5
1.1 The Need for ACCESS 6
1.2 Highlights of ACCESS Science 8
1.3 Scientific Community Support for ACCESS 9
2. Current State of Cosmic-ray Observations and Theory 9
2.1 Observations of Cosmic-ray Energy Spectrum and Composition. 9
2.2 Knowledge of Cosmic-ray Composition 11
2.3 Shock Acceleration in Supernova Remnants (SNR) 11
2.3.1 General Description of SNR Shock Acceleration Models 11
2.3.2 Predictions of SNR Shock Acceleration Models 12
2.3.3 Existing Data Suggest Inconsistency with SNR Shock Models 13
2.4 Cosmic Rays in the Galaxy 14
2.4.1 Cosmic-ray History in the Galaxy 14
2.4.2 Secondary Nuclei Observations with ACCESS 16
2.4.3 Energy Loss by Electrons 17
2.4.4 Value of Measuring Electron Spectrum 18
2.5 Source Material of Cosmic Rays 19
2.6 Connection to Higher-energy Processes 20
2.6.1 Air Shower Studies 21
2.6.2 Underground Studies 22
2.6.3 Link to the Highest Energies 23
3. Measurement Requirements 24
3.1 Scientific Objectives for ACCESS 24
3.1.1 Category A Objectives 24
3.1.2 Category B Objectives 24
3.2 Instrument Concept 24
3.2.1 Ionization Calorimetry 25
3.2.2 Transition Radiation Detector 26
3.3 Measurements Required to Meet Scientific Objectives 28
3.3.1 Category A 28
3.3.2 Category B 29
4. ACCESS: Baseline Instruments and Payload Support and Interface Module 29
4.1 Payload System Overview 30
4.2 Calorimeter 30
4.3 Transition Radiation Detector 31
4.4 Payload Support and Interface Module 32
4.4.1 Structure 32
4.4.2 Thermal 35
4.4.3 Power 37
4.4.4 Command and Data Handling 37
4.4.5 Extravehicular Robotics and Crew Interfaces 39
5. Mission Plan 40
5.1 Mission Description 40
5.2 Mission Requirements Flow-down 40
5.3 Mission Timeline 42
5.3.1 STS Launch and ISS Docking 42
5.3.2 Instrument Activation and Major Scheduled Events 43
5.3.3 De-activation and Retrieval 44
5.4 Mission Operations Concept (Including Ground Operations) 44
5.5 Mission Data Products 45
References 46
Acronyms 47

Executive Summary

ACCESS, the Advanced Cosmic-ray Composition Experiment for the Space Station, will directly address the most fundamental questions about cosmic rays - Where do they come from? What are they made of? How are they accelerated? It will test, and distinguish among, theories of cosmic-ray origin by measuring the individual-element composition of the cosmic rays at energies a thousand times higher than any previous measurements of similar resolution - reaching to 10^{15} eV.

ACCESS combines several well-established techniques of charged-particle identification in a 5500 kg detector system with a 6 m^2 aperture. It takes advantage of the capability of the International Space Station (ISS) to accommodate large, massive payloads and orient them toward the zenith. ACCESS will be carried into orbit on the Space Shuttle and transferred onto the ISS truss, where it will operate for three to four years before being returned to the ground on the Shuttle.

ACCESS is one of the initiatives recommended for the decade 2000 - 2010 in the decadal report (released May 2000) of the Astronomy and Astrophysics Survey Committee of the National Research Council, and it has been identified as a priority mission for the near term in the 2000 Strategic Plan of NASA's Office of Space Science.

A project formulation study, the results of which are described in this document, and an earlier accommodation study have demonstrated the feasibility of building ACCESS and operating it on the ISS. The technology for this mission is in hand, and the formulation study is on track for the release in early 2001 of an Announcement of Opportunity to propose for building the instruments, in anticipation of placing ACCESS onto the ISS in 2007.

1. Introduction

The origin of cosmic rays is one of the major unsolved puzzles in astrophysics. Their source and full nature are still undetermined, despite the fact that cosmic rays were one of the first forms of radiation from space to be discovered.

While there are good reasons to believe that cosmic rays are intimately connected with the enormous release of energy in supernovae explosions, **some cosmic rays have energies a million times larger than the most powerful supernova explosion can produce,** and a billion times larger than any man-made accelerator.

Pioneering measurements have indicated already that the supernova acceleration theory for the origin of cosmic rays cannot account for all observations. The fact that the power-law spectrum of cosmic-ray intensity with energy continues with a nearly continuous slope for five orders of magnitude above the highest energies thought possible for production in supernovae seems in direct conflict with this popular theory (Figure 1).

At low energies, we know that cosmic rays consist of essentially all the elements in the periodic table, with proportions similar to those measured in the local Galaxy. **We must extend this level of detailed understanding of composition higher in energy, into the energy region where our present ideas about supernova acceleration of charged particles begin to fail.** The exact nature of the variation of the chemical composition of cosmic rays with energy has proven to be an essential component for progress — this extra dimension adds the analog of color to an otherwise monochrome energy spectrum.

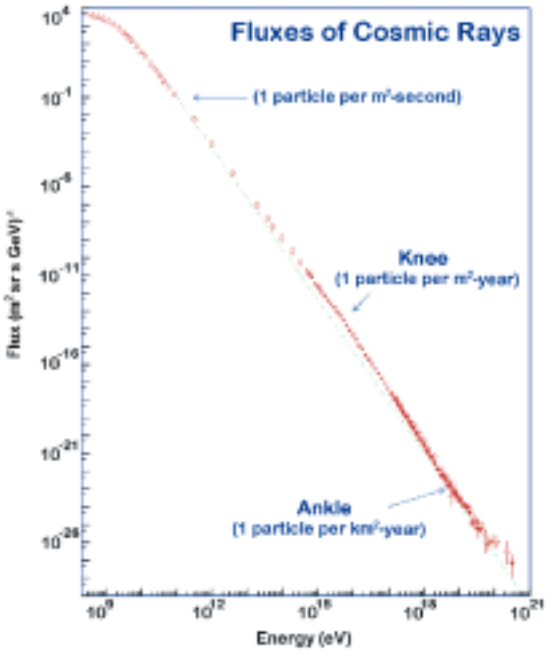

Figure 1. Flux of all cosmic rays vs. total energy per particle. The region around 10^{15} eV is referred to as the "knee" because the shape of the spectrum changes there.

This is the purpose of ACCESS (Advanced Cosmic-ray Composition Experiment for the Space Station). **ACCESS is directed at measuring cosmic rays to the supernova energy scale of 10^{15} eV to address directly three fundamental questions about cosmic rays:**

- **Where do they come from?**
- **What are they made of?**
- **How are they accelerated?**

Because the number of cosmic rays decreases rapidly with energy, data with good charge resolution now exist only up to 10^{12} eV. An instrument probing the high-energy region needs to be large and operate for several years. **ACCESS will have a collecting power more than a hundred times larger than previous experiments.** This power is complemented by excellent individual resolution of elements, from hydrogen to nickel nuclei.

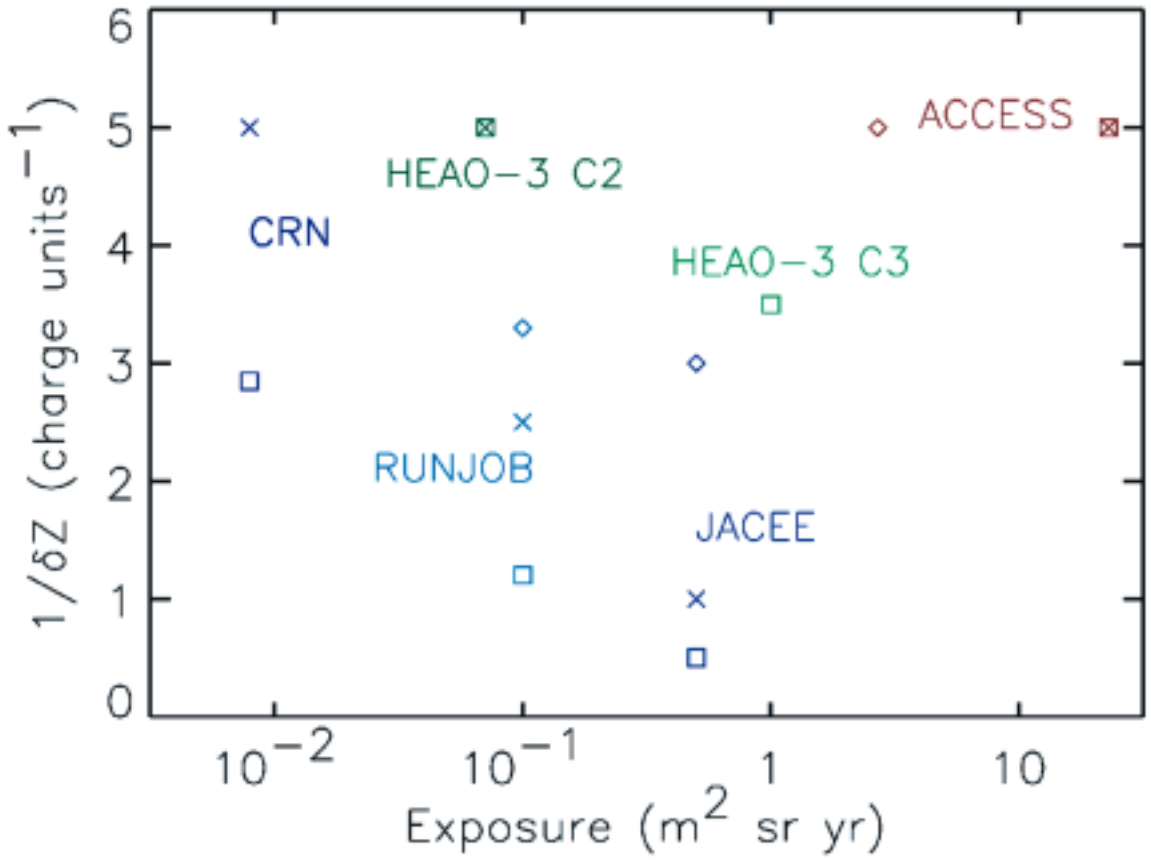

Figure 2. ACCESS has a better combination of element resolution and exposure than previous measurements of high-energy cosmic rays. Symbol key: diamond=hydrogen, x=oxygen, square=iron

Figure 2 indicates the extent to which ACCESS will exceed previous instruments in the combination of charge resolution (needed for element identification) and collecting power (or exposure). **ACCESS takes advantage of the inherent capability of the International Space Station (ISS) to accommodate large, massive payloads** (Figure 3). The deployment of ACCESS on the ISS for three to four years will provide the needed measurements of cosmic-ray particles into the energy region of the supernova scale.

1.1 The Need for ACCESS

To date, most of the data on cosmic rays above 10^{14} eV come from ground-level observations of air showers, showers of secondary particles produced when very energetic cosmic rays hit the Earth's atmosphere. These measurements have established the shape of the overall cosmic-ray energy spectrum but do not establish the identity of the primaries initiating the shower. The best these measurements can do is to indicate the mean atomic weight. Without identification of specific elements in the primary cosmic rays, one cannot directly test composition changes predicted by supernova models, and one cannot distinguish between contributions of primary accelerated nuclei and secondary nuclei produced by fragmentation in the interstellar medium. **ACCESS will provide the direct identification of individual elements that is required.**

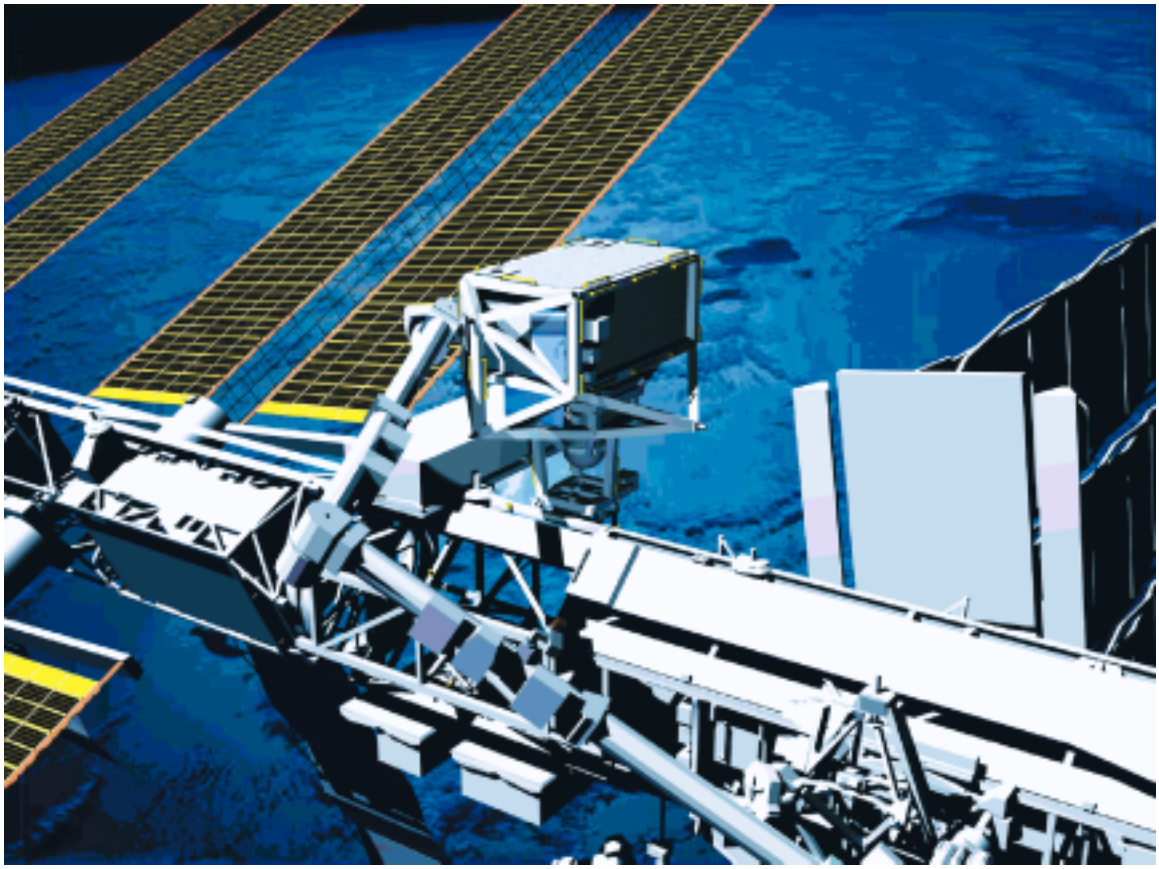

Figure 3. Artist's conception of ACCESS attached to the International Space Station

Balloon flights have begun to reveal the spectra of cosmic-ray hydrogen and helium up to around 10^{14} eV, but these results at high energies have seriously limited statistical accuracy. Direct observations of energy spectra up to 10^{15} eV can only be done with larger instruments and substantially longer exposure times. The region between 10^{14} and 10^{15} eV is critical, because models of cosmic-ray acceleration by supernova shocks lead us to expect changes in the elemental composition of the cosmic rays in just this interval. No electronic detector of cosmic rays has yet combined both the capability of measuring such high energies and the duration of exposure needed to determine cosmic-ray composition. **ACCESS will, for the first time, provide direct measurements of the energy spectra of individual elements in the cosmic rays over several orders of magnitude of energy, up to 10^{15} eV.**

Figure 4 shows the energy reach of ACCESS and of previous instruments that had charge resolution capable of distinguishing individual elements. This figure demonstrates that, for hydrogen and helium, ACCESS will increase the energy to which cosmic-ray elements are measured by a factor of about five; and for heavier elements ACCESS will increase the energy to which individual elements are measured by roughly a factor of one hundred.

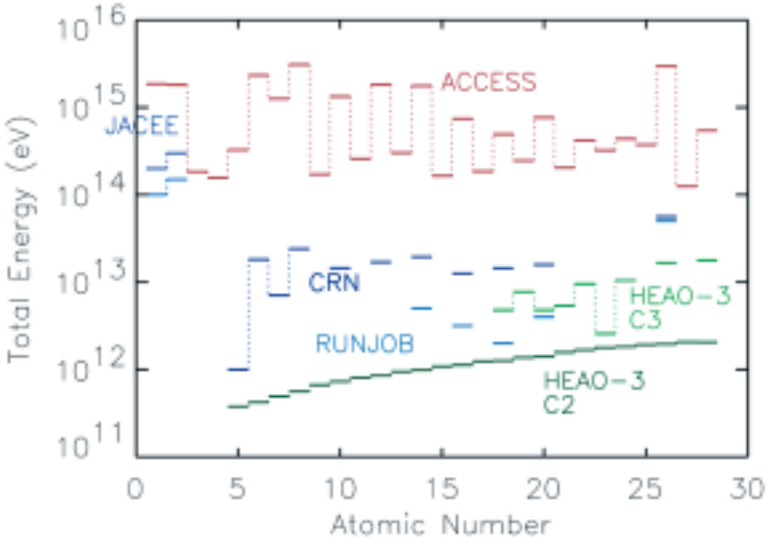

Figure 4. Maximum energy reached vs. atomic number for ACCESS and for previous measurements with individual-element resolution. For points representing previous measurements, a consistent definition of "maximum energy" has been imposed: the lower of (a) the energy at which ten events of the given atomic number are identified, or (b) the energy at which the particular instrument can no longer measure energy. For ACCESS, the ten-event limit is predicted assuming a spectrum unbroken from that observed at lower energies.

1.2 Highlights of ACCESS Science

ACCESS will test the validity of supernova shock theory of cosmic-ray acceleration by observing changes in the composition of the cosmic rays at increasing energy. Some changes that earlier measurements have indicated seem to be inconsistent with the simple supernova model. Other changes - differences between the spectra of hydrogen and of heavier elements in the interval 10^{14} to 10^{15} eV - are expected from present data but have not yet been observed. (See Section 2.3.)

ACCESS will measure how high-energy cosmic rays escape from the Galaxy. Cosmic rays are partially trapped by the galactic magnetic field, and this confinement mechanism changes the cosmic-ray energy spectrum, i.e. the number of cosmic rays measured at different energies. Theories of cosmic-ray acceleration predict the spectral shape of the cosmic rays at their source, not the energy spectrum observed near Earth. Only by understanding the confinement can one determine with which energy distribution the cosmic rays are produced originally. (See Section 2.4.)

ACCESS will distinguish between theories describing the cosmic-ray seed population, which is the origin of the particles that get accelerated to cosmic-ray energies. This is achieved by measuring the abundances of rare elements. At high energies, the measured abundances can more easily be related to the source abundances than can be done at lower energies, because they have undergone fewer collisions in interstellar space. The relative abundances of the seed population provide a "fingerprint" that can help identify their source. (See Section 2.5.)

ACCESS will establish benchmark cosmic-ray composition measurements that must be accommodated by the particle interaction models used in analysis of data from ground arrays observing air showers. The determination of composition from the ground array data depends heavily on these models. The direct measurements of ACCESS, overlapping in the 10^{14} - 10^{15} eV region with the ground array data, will rule out some interaction models and allow others. (See Section 2.6.)

1.3 Scientific Community Support for ACCESS

ACCESS is one of a small number of space-based "small initiatives" for the decade 2000-2010 for which **approval and funding are recommended in the decadal report of the Astronomy and Astrophysics Survey Committee of the National Research Council,** ***Astronomy and Astrophysics in the new Millennium*** (National Academy Press, 2000). That report places ACCESS among the **"exciting opportunities where a relatively small investment will potentially leverage an enormous gain in capability and scientific return."** It notes that ACCESS "will measure the spectrum and composition of cosmic rays with energies up to 1000 TeV. This experiment will provide unique data for studying where the cosmic rays originate and how they are accelerated." (1 TeV = 10^{12} eV)

ACCESS has been identified as a priority mission for the near term in the 2000 Strategic Plan of NASA's Space Science Enterprise. (NASA report in press.) One of the three "quests" of the Structure and Evolution of the Universe (SEU) theme of OSS (NASA's Office of Space Science) is "To explore the cycles of matter and energy in the evolving universe." In the context of its quests, the SEU theme has developed six focused research "campaigns", including "Understand the cycles in which matter, energy, and magnetic field are exchanged between stars and the gas between the stars." *(Cosmic Journeys - To the Edge of Gravity, Space, and Time — Structure and Evolution of the Universe Roadmap: 2003 - 2023*, roadmap document for the SEU theme, NASA OSS, September 1999.) A key process in the cycles of matter and energy is the explosion of supernovae. Measurement of the elemental composition and energy spectra of cosmic rays by ACCESS will test the limits of the supernova remnant shock model, in which a substantial fraction of the energy of these exploding stars is imparted to the cosmic rays.

The objectives of ACCESS are among the priority objectives described in two committee reports of the National Research Council (National Academy Press, 1995) — *Opportunities in Cosmic-Ray Physics and Astrophysics*, the report of the Committee on Cosmic-Ray Physics; and *A Science Strategy for Space Physics*, report of the Committee on Solar and Space Physics.

2. Current State of Cosmic-ray Observations and Theory

2.1 Observations of Cosmic-ray Energy Spectrum and Composition

Figure 1 showed the differential energy spectrum (nuclei per m^2-sr-s-GeV, 1 GeV=10^9 eV) of all cosmic-ray nuclei from below 10^9 eV to above 10^{20} eV. Between several times 10^9 eV and a few times

10^{15} eV, the spectrum falls as a smooth power law of (energy)$^{-\alpha}$ where α is approximately 2.7. Between this "knee", at a few times 10^{15} eV, and the "ankle", at a few times 10^{18} eV, the spectrum falls more steeply, with α about 3.0. At the highest energies the spectrum is not so steep, and recent results (Takeda et al. 1998) demonstrate that the spectrum extends to several times 10^{20} eV. The existence of these highest-energy cosmic rays is contrary to the expected cutoff just below 10^{20} eV (Greisen 1966; Zatsepin & Kuz'min 1966), due to the rapid loss of energy from photoproduction of pions in the interaction of protons above 5 x 10^{19} eV with the microwave background photons.

To date, most of the data on cosmic rays above 10^{14} eV comes from ground level observations of air showers, which measure the energies of the incident cosmic rays but do not determine their elemental identity.

The best data to date on the high-energy spectra of hydrogen and helium in the cosmic rays come from the series of balloon flights from 1979 through 1994 of the Japanese-American Cooperative Emulsion Experiment (JACEE). They observed a total of ten H above 200 TeV, and ten He above about 300 TeV. (Asakimori et al. 1998). Similar results come from the RUssian Nippon JOint Balloon (RUNJOB) experiment (Apanasenko et al. 1999).

The best data to date on the high-energy spectra of individual elements heavier than He in the cosmic rays come from a gas Cherenkov and transition radiation detector system, which had about 3 days of net exposure in orbit on the Space Shuttle in 1985 (Müller et al. 1991). That instrument gave individual-element measurements of C, O, Ne, Mg, and Si, and measurements of the "Fe-group" to about 30 TeV. It also measured the secondary element B and the element N to about 2 to 3 TeV (Swordy et al. 1990). Spectra of heavier secondary nuclei, K, Sc, Ti, and Cr, relative to Fe, were measured on HEAO-3 up to ~10 TeV (Binns et al. 1988). The JACEE project extended measurements of charge groups CNO ($6 \le Z \le 8$), Ne-S ($10 \le Z \le 16$), and Fe-group ($Z > 17$) (where Z is atomic number) to higher energies, observing ten CNO nuclei with energy greater than 3 x 10^{14} eV, and similar numbers of the other two charge groups above a somewhat lower energy (Takahashi 1998). The RUNJOB experiment reported similar results for Fe and for the CNO and NeMgSi groups. Also, BACH, a balloon-borne instrument detecting Cherenkov light produced in the atmosphere by incident cosmic rays, reported a measurement of the flux of iron nuclei between 3 x 10^{13} and 1 x 10^{14} eV (Seckel et al. 1999). (For measurements where the individual incident cosmic-ray nuclei are observed, results are usually expressed as energy per nucleon; but here we use energy per nucleus (energy per nucleon multiplied by atomic mass) in order to connect to the air-shower data, where the incident nuclei are not identified and only the total energy per nucleus is measured.) **These earlier data leave a substantial gap in our knowledge of the cosmic-ray composition, and this gap falls in an energy regime where measurements of the composition will test theories of cosmic-ray origin.**

2.2 Knowledge of Cosmic-ray Composition

Broadly speaking, results from these early measurements indicate that the elemental composition of the cosmic rays is similar to that of the interstellar material that made the solar system. There are two notable exceptions to this general statement.

First, some elements, for instance, Li, Be, and B, which have almost negligible abundance in the solar system, are not nearly so rare in the cosmic rays. This fact is understood as the result of spallation of heavier cosmic rays that suffer nuclear interactions with the ambient interstellar gas. These spallation products are referred to as secondary cosmic rays, to distinguish them from the primary cosmic rays that are originally accelerated in the cosmic-ray source. Their relative abundances give a direct measure for the pathlength through which cosmic rays propagate during their journey through the Galaxy. It has been observed that this pathlength decreases with energy. As a consequence, the energy spectra of primary and secondary cosmic rays are different. In turn, the spectra of primary cosmic rays have a considerably different shape when they arrive at Earth, as compared to when they are generated at their sources. **It is essential to measure this difference to the highest energy possible in order to understand how the galactic propagation affects the primary cosmic rays. Without that understanding, the relationship between the observed primary spectrum and the spectrum at the cosmic-ray source is not known, so one of the principal predictions of any cosmic-ray source theory cannot be tested.**

A second difference between the cosmic-ray and solar-system elemental composition - a difference among primary cosmic rays - is that elements of lower first-ionization potential (FIP) are more abundant in the cosmic rays relative to the solar system than are elements of higher FIP. Alternatively, the same difference can be described as a greater abundance of refractory elements - those that are more likely to be found in interstellar dust grains. Distinguishing between these two descriptions of the differences requires measuring primary abundances of elements whose primary component has not yet been well determined. For some elements (e.g. Na) at moderate energies (several GeV/nucleon) at least two-thirds of the observed cosmic rays are secondaries, so inference about the primary abundances is quite uncertain. But because secondary cosmic rays have a steeper energy spectrum than primaries, **at high energies accessible to ACCESS these elements in the cosmic rays will be almost entirely primary, thereby permitting an unambiguous determination of their source abundance.**

2.3 Shock Acceleration in Supernova Remnants (SNR)

2.3.1 General Description of SNR Shock Acceleration Models

The supernova shock theory of cosmic-ray acceleration builds simply on the basic notion that a collisionless shock, traveling through a medium in which charged particles can diffuse, will give a great deal of energy (actually momentum) to those few particles that diffuse back and forth through the shock many times before being convected away. The momentum gain that arises on each crossing due to repeated scattering off of magnetic irregularities

that are converging is proportional to the momentum the particle already has; hence the resulting momentum is an exponentially increasing function of N, the number of times the particle crosses the shock. The probability that a particle will return to the shock at least N times from downstream is an exponentially decreasing function of N. The combination of these two facts tells us that the particles will leave the shock with a power law distribution in momentum. In the linear, or test-particle, approximation the exponent of this power law depends on the ratio of the speed of the shock to the speed of sound, or the Alfvén speed (the Mach number). This process will end when the particles reach the momentum above which the system (magnetic fields and plasma) can no longer contain the particles in the vicinity of the shock.

2.3.2 Predictions of SNR Shock Acceleration Models

Linear theory: Supernova cosmic-ray origin theories predict that the produced particle spectrum should cut off exponentially in the region 10^{14} - 10^{15} eV per unit charge. This cutoff depends on the speed of the shock (which in turn depends on the parameters of the space in which the supernova shock expands, such as gas density and temperature) and on the local magnetic field strength, which also affects the shock speed. The ambient magnetic field affects the shock strength by determining the Alfvén speed and hence the Mach number. Also, a higher magnetic field keeps the particles in the accelerator longer, and hence a higher energy can be reached. With typical values of parameters for a supernova shock — shock size 10 pc, shock velocity 4500 km/sec, magnetic field 3 μg — we can estimate (Hillas 1984) that the maximum energy to which the supernova shock can accelerate a nucleus of charge Z is Z x 1.5 x 10^{14} eV. It is interesting to note that detailed computer simulations of supernova shock acceleration give upper limits quite close to these values.

Furthermore, the slope of the spectrum also depends on these parameters. Large Mach number shocks are stronger and produce flatter spectra of accelerated particles. Therefore, a higher magnetic field weakens the shock (Mach number is smaller), so the slope is steeper. A higher gas density increases the Mach number (slower sound speed); and a higher temperature decreases the Mach number (higher sound speed). Thus, we see that local effects can influence the overall slope of the spectrum and the upper energy limit of the acceleration process.

Non-linear theory: The non-linear theory of shock acceleration takes account of the fact that if a shock is efficient in accelerating particles, a considerable fraction of the shock's energy will wind up in the form of energetic particles that will, in turn, affect the structure of the shock, namely: the shock transition will be broadened and the compression ratio can be much larger than in the linear theory, resulting in much harder production spectra. Also the momentum spectrum will no longer be a simple power law, but the resulting distortion in the momentum spectrum is maximal at only a few GeV and therefore not in the energy range of ACCESS. However, the harder production spectrum could be observed if the effects of galactic propagation can be determined. As discussed in Section 2.2, ACCESS is well suited to make this determination.

There are other effects of this nonlinearity that have a bearing on other fields of high-energy astrophysics. Cosmic-ray production in young supernova remnant shocks is expected to be efficient and strongly nonlinear, since 5% to 10% of the total ejecta kinetic energy is required to replenish cosmic rays as they escape from the Galaxy. The heating of the gas to X-ray-emitting temperatures is strongly coupled to the acceleration of cosmic-ray electrons and ions. Whatever energy goes into cosmic rays comes out of the thermal gas. In nonlinear, diffusive shock acceleration, compression ratios will be higher, and the shocked temperature lower, than test-particle, Rankine-Hugoniot relations predict. The density and temperature are the two critical parameters for X-ray line models. All predictions of the ejecta composition (a fundamentally important result from spacecraft like Chandra) depend strongly on these parameters. Despite the expected efficiency of shock acceleration, virtually all current X-ray line models assume that the shocks that heat the gas do not place a significant fraction of their energy in cosmic rays (exceptions to this are Chevalier 1983 and Dorfi & Bohringer 1993). If shocks accelerate cosmic rays, X-ray models must include this.

2.3.3 Existing Data Suggest Inconsistency with SNR Shock Models

If the spectra of all accelerated particles were plotted in units of energy-per-unit-charge, considerations from linear and non-linear theory alike indicate that the spectra of the nuclei should all be the same in shape. However, when viewed in units of total energy, the higher-charged nuclei should extend to higher energy (i.e. a factor of 26 for iron over hydrogen). Thus, if there were an exponential cutoff, the chemical composition of the cosmic-ray beam should become progressively heavier as we look higher in energy approaching 10^{15} eV.

Unfortunately, indirect (air shower) measurements to date in the 10^{14} - 10^{16} eV (total energy) region show no evidence for exponential cutoffs. Rather, there appears to be a gradual steepening of the spectrum from a spectral index of 2.75 to ~3.0, with only indirect evidence that the mean mass of the particles is increasing. **There appears to be, therefore, a serious gap between theoretical models of cosmic-ray acceleration/propagation and observations.** Direct measurements of the chemical composition of cosmic rays in this energy region would greatly advance our understanding of these processes.

It should be pointed out that if the spectrum of He and heavier ions is flatter than that of H, as is suggested by current data at high energy (Figure 5), then there is serious disagreement with the simple theory of cosmic-ray acceleration in SNR shocks. Figure 6 shows the statistics that ACCESS would achieve in testing the validity of the spectral differences suggested by the data of Figure 5. **ACCESS will improve on the existing data by going to higher energy, by improving the statistics at energies that have been measured, and by separately measuring individual elements rather than measuring only element groups.**

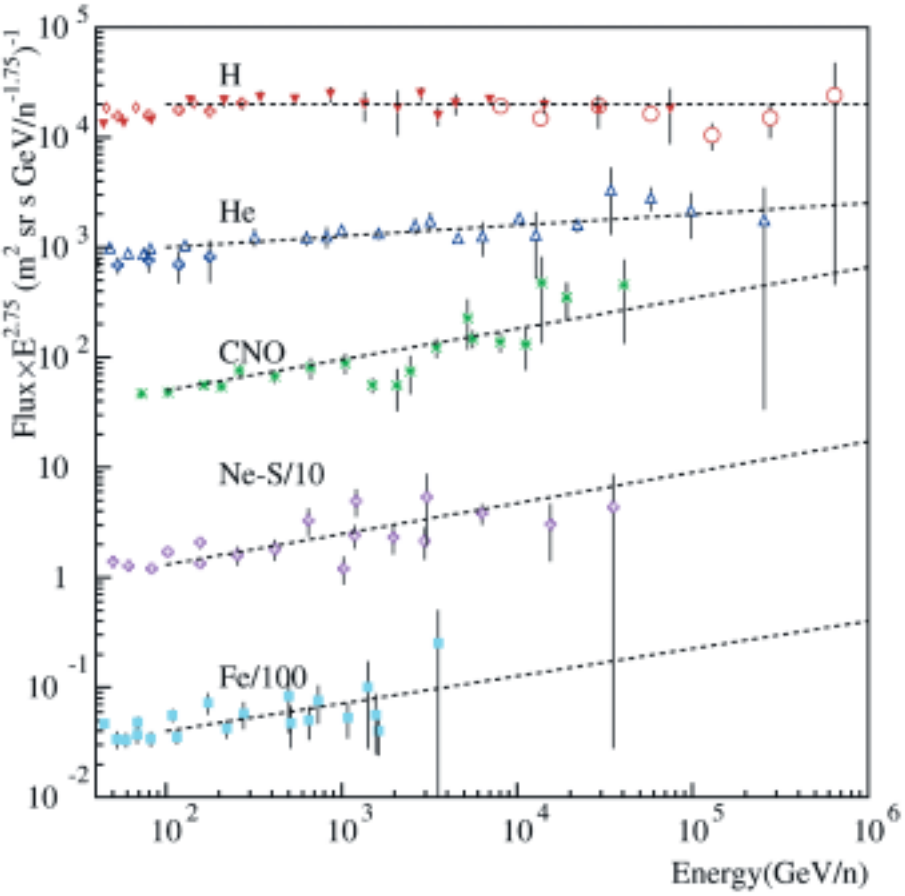

Figure 5. Summary of existing data for flux vs. energy of cosmic rays. Note that the flux scale has been multiplied by $E^{2.75}$, so the steeply falling spectra appear roughly flat in this figure. Note that CNO and Ne-S measurements at the higher energy were for element groups; individual elements were not resolved.

2.4 Cosmic Rays in the Galaxy

2.4.1 Cosmic-ray History in the Galaxy

The detailed composition of cosmic rays arriving at Earth has been studied for many years. With ACCESS we examine how elemental composition at the highest energies can be used to investigate a favorite paradigm — that of diffusive shock acceleration by supernova remnants. **To derive the nature of the sources from the measurements made near Earth, one needs a detailed understanding of the history of cosmic rays during their passage through our Galaxy.** This process is often referred to as propagation, but this is really something of a misnomer since there are reasons to believe that cosmic rays may also be accelerated during this process by the general magneto-hydrodynamic turbulence of the Galaxy.

The discovery, nearly 30 years ago (Juliusson et al. 1972; Smith et al. 1973), of an energy dependence to the apparent "propagation" pathlength of cosmic rays prompted the realization that the measured cosmic-ray energy spectra are significantly steeper than would be observed near the source. The observed fraction of secondary nuclei produced by spallation in the

Galaxy declines with increasing energy, indicating that the average amount of material encountered by cosmic rays decreases with increasing energy. From these measurements, the cosmic rays at energies of ~100 GeV/nucleon pass through only 20% of the galactic material that those of several GeV/nucleon experience. The present interpretation of this effect is that particles at higher energy more easily escape from the Galaxy.

Observations of cosmic-ray fluxes at Earth reveal the equilibrium population of a balance between the source production and losses from either direct spallation or escape from the galactic plane. We therefore observe fewer particles at high energies than are produced in the sources because of increased losses from the Galaxy itself. But this presents something of a puzzle. We know from air-shower measurements that the overall cosmic-ray spectrum extends up to energies in excess of 10^{20} eV in a more or less constant power-law form, over many orders of magnitude. Does this mean the escape length from the Galaxy also declines over this entire energy range? This seems unlikely, since a simple extrapolation of this behavior into the "knee" region, near 10^{15} eV, makes the apparent escape length comparable to the thickness of the galactic plane - yet no significant anisotropies are seen in the arriv-

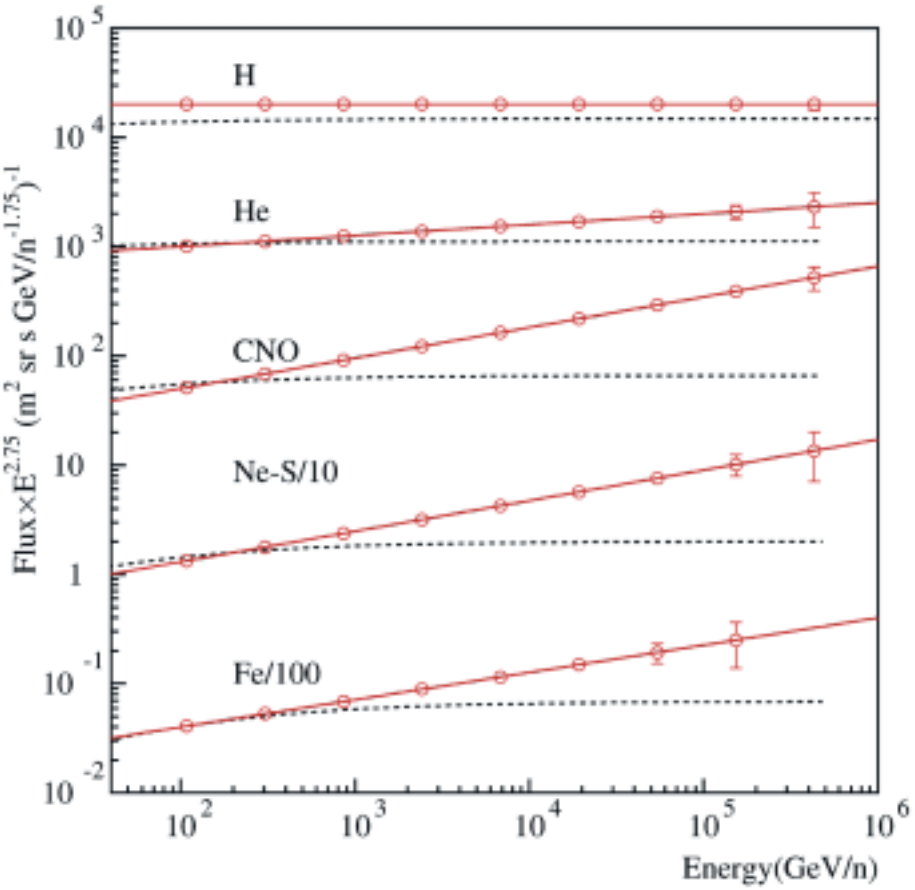

Figure 6. Expected statistical uncertainties of ACCESS measurements if spectra actually extrapolate as shown in Figure 5. The dashed lines show the expected fluxes for these groups if all nuclei have the same rigidity spectra at the source as hydrogen.

ing cosmic-ray fluxes at these, or higher, energies. This issue remains a mystery.

2.4.2 Secondary Nuclei Observations with ACCESS

Our direct knowledge of the source spectra and history of cosmic rays in our Galaxy is limited in scope to the energy ranges where the energy dependence of the escape length is known. Unfortunately these measurements only extend to energies of ~100 GeV/nucleon, far lower than the highest energy direct measurements and eight to ten orders of magnitude below the highest energy cosmic rays observed through air showers.

It is essential to extend to the highest energy possible measurements that reveal this history. This is one of the key scientific goals of ACCESS since the actual source spectrum of cosmic rays cannot be deduced without these measurements. Although there have been many measurements of the secondary spallation-produced nuclei in cosmic rays, the best observations were made by the HEAO-3 satellite during the 1980s (Binns et al. 1988; Englemann et al. 1990). These data have, by far, the highest statistics of any measurement and, at least in the case of the Cherenkov counter measurements, a well-calibrated energy scale. They also have excellent charge resolution, which is vitally important for good separation of secondaries from neighbors that are predominantly primary in nature.

The data from this satellite for the boron/carbon ratio are shown in Figure 7, together with other data, albeit with lower statistics. Also shown on this picture are simple propagation models based on an asymptotic power law of magnetic rigidity ($\sim R^{-\alpha}$) -dependent escape from the Galaxy. As can be seen, all of these models provide a reasonably good fit to data at these lower energies. Similar fits can be made to the sub-Fe/Fe ratio using the same models. If re-acceleration (i.e., further acceleration of cosmic rays while they are propagating in the interstellar medium) is significant at all energies, the highest energy particles should have the longest pathlengths — since the energy (rigidity) would be expected to increase with residence time in the region where re-acceleration occurs. The absence of this trend from these secondary-to-primary ratios provides constraints on the amount of re-acceleration that could occur over this rigidity range. The "weak limit" of re-acceleration (Seo & Ptuskin 1994), where, asymptotically, $\alpha \sim 0.33$, gives a steeper B/C ratio at lower energies; however, it displays a much flatter dependence on energy in the energy region over which ACCESS will operate. This is due to the competition between the acceleration rate and escape from the Galaxy. The acceleration rate decreases going to higher energy, while the escape rate increases at higher energy.

The expected quality of the ACCESS measurements of the ratio of the secondary boron to the primary carbon nuclei is shown in Figure 7. The "data" points above 700 GeV/nucleon illustrate the statistical uncertainties of the observations that ACCESS would make for the two extreme models. It is obvious that ACCESS will be able to distinguish clearly among these models.

Since the flux of nuclei produced as secondaries in the Galaxy declines even more steeply with energy than the primary cos-

mic rays, the extension of these measurements to higher energies requires huge collecting power. ACCESS, with its several m^2 years of collecting power, will be capable of extending measurements of secondary fluxes by two orders of magnitude in energy. This is a key cosmic-ray measurement, which only ACCESS will be able to provide. Although long and ultra-long duration atmospheric balloon flights can be expected to contribute better elemental measurements in the near future, these will have limitations for measuring secondary nuclei. The overburden of atmosphere for a high-altitude balloon becomes comparable with the thickness of galactic material experienced by these particles at energies of ~1 TeV/nucleon. Since ACCESS is above the atmosphere, it can accurately measure the small fraction of secondary nuclei at the highest energies. Since the propagation pathlength is not expected to decline with a constant rigidity dependence into the multi-TeV region, ACCESS has the power to make a major contribution to our understanding of cosmic rays by these measurements.

2.4.3 Energy Loss by Electrons

Electrons are the only component of the cosmic radiation for which there is direct evidence (synchrotron X-rays) of acceleration in supernovae (Allen et al. 1997). The highest energy measurements of the cos-

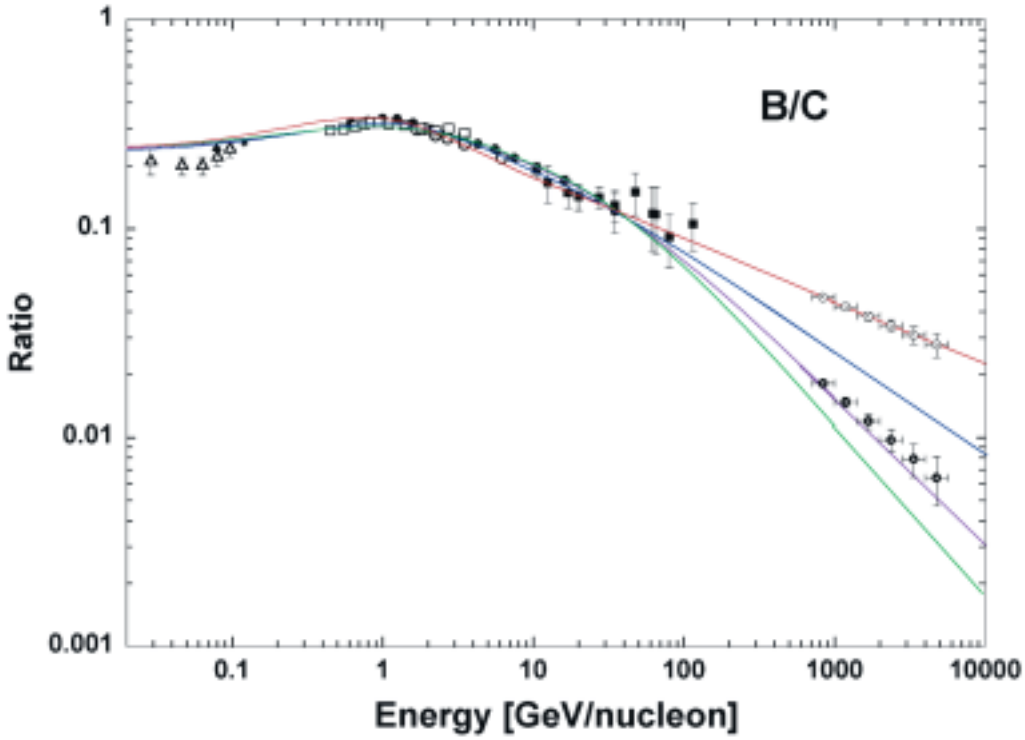

Figure 7. Existing data for the boron/carbon ratio with several theoretical curves that are generally consistent with these data. The "data" points above 700 GeV/nucleon demonstrate the statistical accuracy with which ACCESS could measure this ratio, for two possible results. ACCESS will have the resolution and the statistical accuracy to distinguish among theories.

mic-ray electron spectrum extend to about 1 TeV. Kobayashi et al. (1999) report 15 electrons above 1 TeV. The electrons are of particular interest, because in transport through the Galaxy they are subject to synchrotron and inverse Compton energy losses that limit the age of high-energy electrons. These loss mechanisms do not affect the nuclear component of the cosmic radiation.

The energy-loss rate for high-energy electrons in the environment of galactic interstellar space is proportional to the square of the electron energy. As a result, cosmic-ray electrons with higher energy will have shorter lifetimes; that is, they cannot retain their high energy. Specifically, the lifetime will depend upon the photon density and magnetic field in the region through which the high-energy electrons are moving. Using typical galactic values of these parameters, one finds that electrons with energy above 1 TeV will have lifetimes of less than 10^5 years. Thus, a high-energy electron observed at Earth will be much younger than lower energy electrons, for which the energy losses are much less severe.

2.4.4 Value of Measuring Electron Spectrum

The transport through the Galaxy of cosmic rays, including electrons, is understood to be a diffusion process. Whatever the value of the diffusion coefficient may be, the limited lifetime of the higher energy electrons dictates that high-energy electrons that reach the Earth will come from a region smaller than that from which low-energy electrons or hadrons reach the Earth. This, plus the certainty that electrons are accelerated to multi-TeV energies in supernovae, opens the possibility of identifying individual sources and determining the diffusion coefficient directly.

Whatever the absolute value of the diffusion coefficient, at some high energy the region of space able to contribute electrons that can reach the Earth will become so small as to contain only a few sources (presumed to be relatively recent supernovae), or possibly even only one. It follows as a consequence that the high-energy spectrum of electrons observed at the Earth should exhibit structure (Nishimura et al. 1980) and, very likely, anisotropy (Ptuskin & Ormes 1995; Nishimura et al. 1997).

As there are only a limited number of candidate source supernovae with ages in the range of 10^5 years or less (see e.g., Kobayashi et al. 1999), measurement of the high-energy electron spectrum and examination of its structure may allow determination of the diffusion coefficient that governs transport of the electrons.

This possibility is illustrated in Figure 8, following Kobayashi et al., which shows current electron flux measurements extending to just beyond one TeV. The "Galactic comp[onent]" curve displays the expected electron flux due to a statistical distribution of galactic supernovae with nominal characteristics, 10^{48} eV energy in electron spectra per supernova; a diffusion coefficient varying as the 0.3 power of energy has also been assumed. In addition, contributions to the electron spectrum by the eight known individual supernovae within one kpc of the solar system have been calculated under the same assumptions. The Monogem and Vela SNRs may contribute structure to the electron spectrum above one TeV. In the case of the relatively young supernova Vela, the fea-

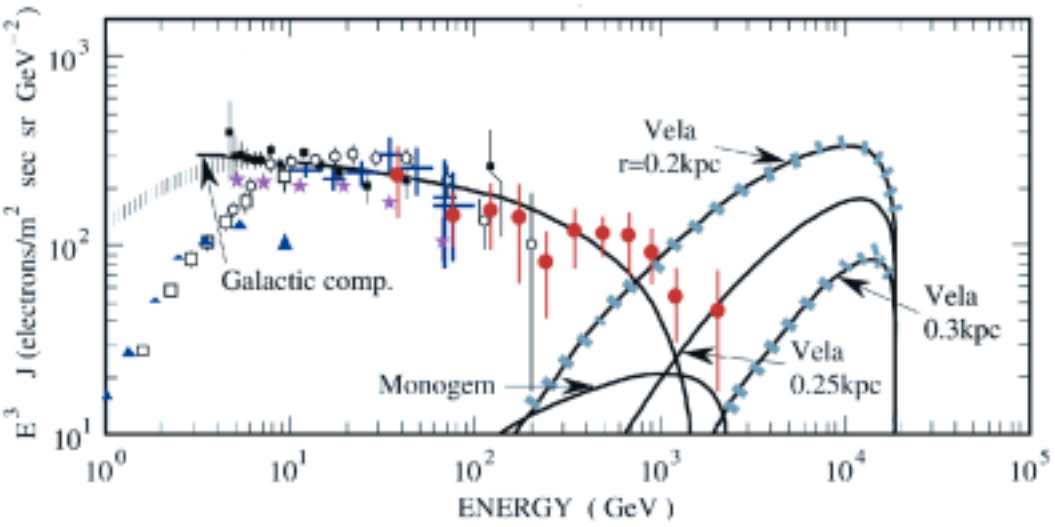

Figure 8. Existing data for cosmic-ray electrons, and expected flux curves showing features in the spectrum due to the Vela and Monogem supernova remnants, with various assumptions about the distance to Vela. Reproduced with permission from 26th ICRC, Kobayashi et al., 1999, and J. Nishimura. Figure edited for clarity.

ture depends sensitively upon the electron diffusion coefficient and distance of Vela. In all cases, the feature becomes prominent in the energy range from one to ten TeV. Measurement of such a feature then allows determination of the diffusion coefficient in that energy range. **Direct determination of the diffusion coefficient, a crucial parameter in understanding the transport of cosmic radiation, has not previously been possible.**

The current electron data present only 15 primary electrons with energy greater than one TeV. An ACCESS exposure of 2 m^2 sr year would increase this to approximately 1500 electrons. In the event that the electron spectral signature of Vela should not be seen, this fact plus the concomitant precise measurement of the end of the electron spectrum would constrain the cosmic-ray diffusion coefficient.

2.5 Source Material of Cosmic Rays

The relative abundances of the elements in the cosmic rays observed near Earth can be extrapolated back to the cosmic-ray source (CRS) by correcting for secondary production during their transport in the Galaxy. The CRS abundances can then be compared with the abundances of ambient material in the solar system (SS), which should be representative of the local galactic abundances. While the CRS and SS abundances are broadly similar, there are distinct differences.

One reasonably successful way of ordering the variations of the ratio CRS/SS is by the FIP of the elements. Elements with FIPs above about 11 eV have a ratio CRS/SS approximately one-eighth that of elements with FIPs below about 9 eV (although hydrogen and helium have even lower CRS/SS). Elements with intermediate FIP have intermediate CRS/SS.

Since the cosmic-ray accelerator is likely to work only on ionized atoms, and easily ionized elements appear to be preferentially accelerated, this correlation suggests that the CRS consists of a partially ionized medium, with a characteristic temperature of ~10^4 K. Meyer (1985) suggested that this partially ionized medium consists of the chromospheres of sun-like stars, from which ions are picked up and accelerated to modest energies by stellar flares. This suprathermal population is then accelerated to high energy by SNR shocks. The observation of just such a FIP-biased preferential acceleration in solar energetic particles and in the solar wind lent credence to this model, although some crucial details remained controversial.

Meyer et al. (1997) argue that the apparent correlation with FIP in the galactic cosmic rays is coincidental, and that the data are better understood by considering the volatility of the elements. In this model, interstellar dust grains near a pre-supernova star are inevitably charged by photo-ionization, and SNR shocks efficiently accelerate these charged dust grains because of their large magnetic rigidity. Ions sputtered from these dust grains are then efficiently accelerated to cosmic-ray energies. As a result, refractory elements, which tend to be found in grains, would be overabundant in the CRS. In addition to the volatility dependence, Meyer et al. expect a mass dependence, particularly for the high-volatility elements. Hydrogen and helium also fit well with the other elements in this model.

The reason that cosmic-ray data fit reasonably well to both the FIP model and the volatility model is that most elements with low FIP are refractory, and most with high FIP are volatile. A few elements break this degeneracy, and measurement of their CRS abundances is particularly important. One such element is $_{11}$Na, which has a low FIP but is semi-volatile. At present, estimates of the CRS abundance of Na are quite uncertain, because at energies where the Na abundance has been measured, a large fraction of the observed Na is secondary, so a substantial correction is needed to get back to the CRS abundance of this element. ACCESS will permit a much cleaner measurement of the CRS abundance of Na because at higher energies the relative flux of secondaries is much reduced (see Section 2.2 and Figure 7).

Other elements that break the FIP/volatility degeneracy include $_{37}$Rb and $_{55}$Cs. If ACCESS can extend its dynamic range for charge identification to include these heavier elements, while retaining a charge resolution of at least 0.25 charge units, then measurement of these elements, which have not previously been resolved, would help distinguish between FIP and volatility as the governing property at the CRS.

2.6 Connection to Higher-energy Processes

Many attempts have been made at determining the mass composition of cosmic rays at high energies, via the study of extensive air showers, the study of the penetrating muon components, or both. At energies beyond the knee, these are in fact the only practical means available. The different techniques used so far have yielded ambiguous and contradictory results. The difficulty stems from the necessity of resorting to modeling to unravel compositional information from the multiplicity of processes taking place. Start-

ing with a primary flux, and assuming a trial composition, the atmospheric cascading processes have to be well understood and simulated to predict observables like the lateral and longitudinal air-shower profiles, or the number and distribution of high-energy muons. Moreover, the atmospheric secondary particles have to be propagated in a realistic fashion, e.g., to deep underground through rock, in the case of some muon measurements.

Each of the elements of the above procedure involves numerous assumptions and uncertainties. For instance, composition studies can be conducted at energies just beyond the knee with measurements deep underground of the multiplicity of muon bundles. In this case, a trial composition is injected into the model calculations (e.g., the primary spectrum is assumed to be dominated by light nuclei, mostly protons, or alternately to be dominated by iron nuclei). But, with the many parameters available to adjust in the models, it is difficult to achieve good sensitivity to the primary composition. Obviously, any reasonable trial composition should be made to agree with the highest energy direct measurements available. **It is therefore crucial to make these direct measurements at energies up to the knee, so as to reduce the number of free parameters for indirect studies at energies beyond the knee.**

2.6.1 Air Shower Studies

Besides the uncertainties in the primary flux and composition, the study and reconstruction of air showers at energies beyond about 10^{14} eV is hampered by insufficient direct knowledge of the hadronic interaction properties of the primary particles with air nuclei and the production of secondary particles at energies above today's collider energies. Therefore, various assumptions and phenomenological models are devised to extrapolate quantities such as interaction cross-sections and pseudorapidity distributions to the relevant energies.

Many of the modern air-shower arrays are equipped with complementary sets of detectors, such as arrays of scintillators, air Cherenkov detectors, and finely segmented hadron calorimeters. The intention is to measure simultaneously as many air-shower parameters as possible, in order to reduce the dependence on models in extracting physically meaningful quantities from the observed shower signals. For instance, the lateral profile of electromagnetic particles (electrons, positrons, and gamma rays), the lateral distribution of low-energy muons, the properties of hadrons near the shower core, and/or the longitudinal development of the air shower are measured simultaneously (at least for a fraction of the events recorded).

When the energy of a primary cosmic ray is reconstructed from the measured shower parameters to determine accurately the shape of the differential energy spectrum, various methods are available, some of which are more or less dependent on an accurate knowledge of the mass composition. In separate analyses, studies of the spectrum in the knee region done by KASCADE and EAS-TOP are made in terms of two components only (protons and iron nuclei), in part because of insufficient direct measurements of the composition at the low edge of their energy reach. Here again, **ACCESS has a vital role to play in providing the requisite composition measurement.**

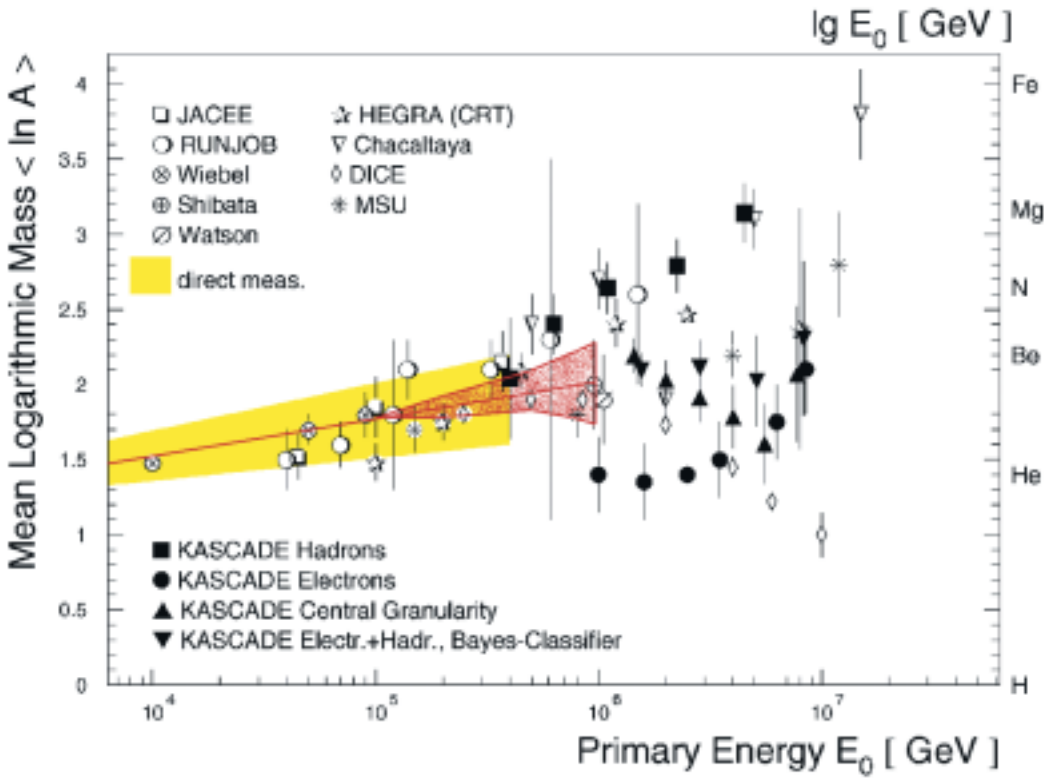

Figure 9. Mean mass of cosmic rays inferred from measurements of cosmic-ray air showers vs. energy of the incident particle. The red region indicates the precision with which ACCESS will determine this quantity.

Finally, the composition-sensitive shower observables are analyzed in an attempt to determine the mean primary mass as a function of energy near the knee region. Figure 9 (Engler et al. 1999) summarizes various analyses, including different signals within the KASCADE experiment itself. It illustrates the wide range of answers that result due to all the uncertainties inherent in these techniques. When direct composition measurements are extended up to the knee, many of these will be reduced.

2.6.2 Underground Studies

Indirect studies of the primary mass composition at energies near and above the knee are also done with experiments deep underground, sometimes in coincidence with an air-shower array at the ground surface. Typically, this is done by measuring the distribution of muon bundle sizes, the separation between pairs of muons, and/or the correlation between muon bundle size underground and shower size at the surface; these quantities are then compared with predictions from model calculations. Here again, various trial compositions are assumed and uncertainties from the details of atmospheric and transport processes affect interpretation of the signal.

As an example, the MACRO detector has been used for such studies, either as a stand-alone instrument (Ambrosio et al. 1992, 1997), or in coincidence with the EAS-TOP air-shower array (Aglietta et al. 1994). Similarly, the LVD detector has

been used in coincidence with the EAS-TOP array (Aglietta et al. 1998). The Baksan underground observatory has also been used as a stand-alone observatory (Bakatanov et al. 1999) for this purpose. Several other measurements have been made, but the few mentioned here are representative. Some of the analyses tend to favor a light composition, dominated by protons and alpha particles at all energies around and beyond the knee, while others point to a composition with an increasingly significant component of heavy nuclei with increasing energy, while others still favor an intermediate mixed composition that remains constant throughout the energy region from below the knee up to about 10^{17} eV. The greatest difficulty in achieving a consistent interpretation is the multiplicity of unknown quantities. **A direct measurement with ACCESS of the mass composition up to near the knee will provide an anchor point to reduce or remove many of the uncertainties that affect the indirect studies conducted with underground detectors.**

2.6.3 Link to the Highest Energies

The study of the spectrum and composition of the cosmic rays at energies from 10^{17} to beyond 10^{20} eV is an endeavor that has been ongoing for several decades now, starting with pioneering efforts such as the Volcano Ranch, Haverah Park, and Yakutsk air-shower arrays, and the Fly's Eye atmospheric fluorescence detector. It continues to this day with new and proposed projects such as AGASA, HiRes, Auger, OWL, and EUSO, to name a few. At these energies, very little is known about the possible acceleration mechanisms taking place and the composition of the cosmic-ray flux.

Composition studies at the highest energies have been conducted by the Fly's Eye collaboration (Bird et al. 1993) by comparing the depth of shower maximum measured with predictions for proton and iron primaries. It is found that an iron-dominated composition agrees best with the measurements at 10^{17} eV, and that the composition becomes progressively lighter with energy, being proton-dominated beyond 10^{19} eV. In contrast, the AGASA collaboration has found (Inoue et al. 1999) no indication of a change of composition over the same energy range, and has found that the composition can be dominated by either proton or iron primaries, depending on the particulars of the model calculations that are used. All the uncertainties that affect indirect studies near the knee become even more problematic with increasing energy, where less is known about the particle interactions. **The reduction of the uncertainties in the model calculations near the knee that will result from ACCESS measurements will help resolve the thorny problem of composition at the highest energies.**

Finally, there has been great interest in formulating models of particle acceleration to the highest energies. For example, it has been proposed that cosmic rays beyond about 3 x 10^{18} eV are extragalactic, and may originate in gamma-ray bursts or AGN (active galactic nuclei) jets. Cosmic rays at lower energies are assumed to be of galactic origin and are dominated by heavy nuclei. This in turn has observable consequences on the flux of high-energy neutrinos from astrophysical sources (Waxman & Bahcall 1998; Bahcall & Waxman 1999). Direct measurements of the composition up to the knee with ACCESS will provide the crucial reference point to determine whether the composi-

tion remains mixed or even becomes heavier beyond the knee, as described above. This would support a galactic origin and will directly affect the assumptions built into the models at the highest energies.

3. Measurement Requirements

3.1 Scientific Objectives for ACCESS

3.1.1 Category A Objectives

These are the primary objectives for ACCESS.

- Test the validity of SNR shock models of cosmic-ray acceleration.
- Determine parameters governing cosmic-ray confinement in the Galaxy
- Measure directly the composition and flux of cosmic rays at energies previously accessible only to indirect (air-shower) measurements, in order to establish benchmark cosmic-ray composition, which must be accommodated by air shower results in the 10^{15} eV energy range.

3.1.2 Category B Objectives

These are scientifically valuable objectives that may be achievable with an instrument that satisfies the Category A objectives.

- Look for evidence of cosmic rays originating in individual supernova remnants.
- Determine the cosmic-ray diffusion coefficient in the interstellar space between a nearby source and the Earth.
- Distinguish among theories for the source of nuclei injected into the cosmic rays.

3.2 Instrument Concept

In order to meet the Category A objectives, ACCESS must determine two quantities for each cosmic-ray particle entering the detector system: the chemical identity, characterized by the nuclear charge Z, and the energy E. The charge measurement is most conveniently derived from the ionization energy loss by the particle in sheets of solid materials, for instance, scintillators or solid-state detectors. The ionization loss increases with Z^2, but for relativistic particles does not depend strongly on E. Thus, provided that statistical and systematic signal fluctuations are sufficiently small, the square root of the ionization loss is a direct measure of Z. While the practical design of such charge detectors requires considerable attention to detail, various solutions are available and have been proven in previous balloon and satellite observations to obtain single element resolution, with an uncertainty in charge assignment of $\delta Z = 0.2$ charge units or better.

The determination of the particle energy is the more challenging task, if stringent limits on the payload mass exist. Two approaches are possible: first, a massive absorber may be used in which the particle interacts, leading to generations of secondary particles, which also are contained in the absorber. Eventually, the entire energy of the particle will be dissipated in the absorber. If the absorber is designed to detect the dissipated energy, then the device becomes a "calorimeter" for the primary particle energy, E. The practical design of such calorimeters will be described below. Calorimeters for cosmic-ray nuclei require hadronic interactions for the primary nucleus and at least some of its fragments, and secondary nucleons. The scale length

(the "nuclear-interaction length") is a rather large quantity and consequently nuclear calorimeters are intrinsically heavy devices.

The situation is different for the second approach in which a measurement of the particle energy is derived from an electromagnetic interaction. Familiar detectors using this principle are magnet spectrometers, Cherenkov counters, or measurements of the ionization loss in gases. All these devices require the particle not to interact hadronically, and to leave a signal that is small as compared to the primary particle energy. This signal typically depends on the particle velocity $\beta = v/c$, but can be related to the E as

$$E = \frac{mc^2}{\sqrt{1-\beta^2}}$$

The devices just mentioned are no longer practical if the particle energy becomes very large, i.e., larger than a few hundred GeV/nucleon. However, transition radiation is another electromagnetic effect that is well matched to the energy region of interest for ACCESS.

ACCESS combines a calorimeter and a transition radiation detector (TRD) in order to span the broadest possible range of atomic numbers and energies. Only the calorimeter is capable of measuring hydrogen and helium at the highest energies, but because of its requirement for large amounts of material in the path of the incident particle, its area must be limited in order to stay within an acceptable total mass. As a result the calorimeter is too small to measure an adequate number of the less abundant heavier elements. The TRD has relatively low mass and so can have a large collecting area, enabling it to see adequate numbers of all the elements heavier than helium. A fraction of the cosmic rays penetrating the TRD will also be measured in the calorimeter, providing a direct intercalibration, for $Z \geq 3$, between two very different methods of measuring energy.

3.2.1 Ionization Calorimetry

Ionization calorimetry provides a method of energy determination for cosmic rays from hydrogen through the heavy elements over a broad energy range. It is a high-energy particle physics analog to the traditional measurement of heat energy with a calorimeter. In an ionization calorimeter, a particle's energy is deposited inside a medium via a cascade of nuclear and electromagnetic interactions. At each step of the cascade the energy of the primary particle is sub-divided among many secondary particles. Ultimately, the primary energy, E_O, of an incident hadron is dissipated via ionization and excitation of the material. The area under the curve of ionization energy versus depth in the absorber provides a measure of E_O, the total energy of the particle. In principal, an infinitely deep calorimeter will provide energy resolution limited only by the statistical nature of the cascade process and the measuring technique. The energy resolution of a finite calorimeter, however, depends on the fluctuations in the energy transferred (inelasticity) to neutral pions, which decay to the gammas that initiate electromagnetic cascades. As a minimum, a calorimeter must measure the energy transferred to electromagnetic cascades in the first interaction. The energy resolution improves as the calorimeter is made deeper, because additional interactions occur, which result in a larger portion of the incident energy

appearing in the electromagnetic component. From Monte Carlo simulations and detailed investigations using accelerators, there is a good understanding of how the energy resolution depends on calorimeter depth, absorber materials, particle species, and primary energy. Calorimetry for measurement of high-energy cosmic rays was pioneered in the Proton series of investigations (Grigorov et al. 1971).

Practical calorimeters for space applications must necessarily be limited in thickness in order to have a reasonable cross-sectional area, i.e. geometrical factor, for collecting the particles. The minimum depth depends on the energy resolution acceptable for a particular experiment. A thin calorimeter to measure the spectra of galactic cosmic rays must meet two basic requirements: (1) the primary nucleus must undergo at least one inelastic interaction; and (2) the energy resulting from the interaction(s) must be measured with good resolution. An optimal thin calorimeter could have a target with thickness of about one proton interaction length located upstream of an electromagnetic calorimeter, which must be sufficiently thick in radiation lengths to develop the electron-photon cascades ensuing from the interactions.

It is important that the target be as thick as possible in interaction lengths, to force interactions of both the incoming primary and the secondary hadrons from that interaction, while remaining thin in terms of radiation lengths, so the cascade development occurs not in the target, but in the calorimeter. The electromagnetic calorimeter should be as thick as possible in radiation lengths to absorb the cascades. It would also be helpful for the calorimeter to be thick in interaction lengths, to force more interactions of the surviving primary and secondary hadrons. Thus, in a practical spaceflight calorimeter, there is a trade-off between maximizing the geometrical factor, (total thickness of the target plus calorimeter (small) and the cross-sectional area (large)) and obtaining the desired energy resolution (large number of radiation lengths).

The ACCESS baseline calorimeter, patterned after the ATIC balloon experiment, is a fully active design composed of BGO (bismuth germanate) scintillating crystals. This BGO calorimeter is located below a carbon target of thickness ~one proton interaction length. Alternate designs under consideration utilize the "sampling calorimeter" concept in which energy detecting layers (e.g. scintillators or silicon detectors) are interspersed between layers of high-Z absorbing material (e.g. Pb or W). Both types, active and sampling, have been used successfully for many years in high-energy physics experiments at particle accelerators.

3.2.2 Transition Radiation Detector

The effect of transition radiation (TR) is related to Cherenkov emission: Cherenkov radiation is emitted when a particle traverses a medium with high speed, while transition radiation occurs when the particle traverses the boundary between two dielectrically different materials. TR has the following features: for highly relativistic particles, most of the emission occurs in the X-ray region; the TR intensity increases with the Lorentz factor, $\gamma = E/mc^2$; and the intensity for a single interface is weak: for a singly charged particle (Z=1), the chance for emission of a photon is of order $\alpha = 1/137$.

In order to make a practical "radiator" for the generation of TR, one usually employs layers of hundreds of thin foils of material, or inhomogeneous materials such as plastic foams, or assemblies of fibrous materials. Then, obviously, the total TR yield increases due to the large number of interfaces, but interference effects between the different interfaces will affect the spectral distribution and lead to saturation of the signal at very high Lorentz factors, $10^4 \leq \gamma_s \leq 10^5$. By careful tuning of parameters such as choice of radiator material, thickness and spacing of foils or fibers, one can obtain practical radiators that provide a γ-dependent TR signal over the Lorentz factor range from $\gamma \approx 500$ to $\gamma \approx 50{,}000$. Over this range then, corresponding to energies of about 500 GeV/nucleon to 50,000 GeV/nucleon (or total energies up to 3×10^{15} eV for iron nuclei, or 0.8×10^{15} eV for oxygen) the magnitude of the TR signal is a measure for the particle energy.

An important fact is the proportionality of the TR signal to Z^2, thus the relative magnitude of fluctuations in the signal becomes smaller for nuclei with large Z. The fluctuations are generally too large for energy measurements of the lightest nuclei, H and He, while measurements of higher charges ($Z \geq 3$) have proven to be successful. At energies below γ=500, the TR signal is too low to be detectable. However, in this region the relativistic rise in specific ionization provides an alternate means of energy measurements with the TRD.

For singly-charged particles, one still can use a TRD as a discriminator between particles of high and low γ values, for instance, electrons and protons of the same energy. Thus, for the observation of cosmic-ray electrons, and the rejection of the abundant proton background, TRDs have proven to be powerful discriminators in balloon experiments since the 1970s. For similar particle identification purposes, TRDs are now also found frequently in accelerator experiments.

TR X-rays are emitted in the direction of the primary particle trajectory. Hence, any detector to observe TR signals will also record a superimposed signal due to the ionization loss of the particle. To minimize ionization signals, one typically employs gaseous detectors, and to maximize the X-ray conversion efficiency, a heavy detector gas such as xenon is needed.

Based on these considerations, the optimum TRD consists of a combination of a radiator with an X-ray detector downstream, as shown schematically in Figure 10. Sandwich arrangements of multiple radiator/detector combinations are commonly used to provide redundancy in the measurement and in order to assess the level of signal fluctuations for each primary particle. The advantage of the TRD approach is the intrinsically low mass/area ratio of such detectors. This makes possible the practical design of very large detectors.

A transition radiation detector designed in this fashion was successfully used for the

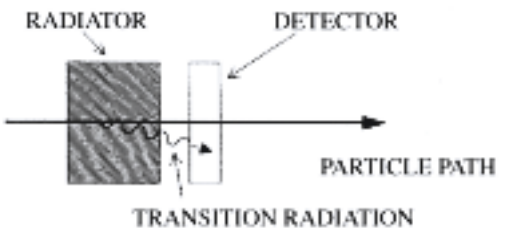

Figure 10. Schematic concept of a generic transition radiation detector

observation of cosmic-ray nuclei in the TeV/nucleon region for the first time in the CRN instrument of the University of Chicago on Spacelab-2 in 1985. CRN, which used multi-wire proportional counters (MWPC) for detecting the X-rays, was enclosed in a pressurized shell. Weight restrictions on ACCESS prohibit the use of such a shell. As it is impossible to operate the MWPCs in external vacuum, the ACCESS baseline design replaces the MWPCs with layers of single-wire proportional tubes. An instrument (TRACER) employing this design successfully verified this approach in a 1999 balloon flight.

An important feature of TRDs is the fact that such detectors can be fully calibrated at accelerators. As the TR effect depends solely on the Lorentz factor γ, accelerator beams of muons, pions, and electrons can cover the entire γ range that corresponds to the energy range covered by ACCESS.

3.3 Measurements Required to Meet Scientific Objectives

3.3.1 Category A

- Measure spectra of $_1$H and $_2$He for energies from 10^{12} to 10^{15} eV. (Extension of these measurements down to 10^{11} eV is desirable because it would provide good overlap with previous measurements.)
- Measure spectra of $_3$Li through $_{28}$Ni from 10^{12} eV/nucleon to as high in energy as their fluxes will allow. Exposure must be great enough to measure spectra of $_6$C, $_8$O, and $_{26}$Fe to 10^{15} eV (energy per nucleus). (Extension of these measurements down to 10^{10} eV is desirable because it would provide good overlap with previous measurements.)

Exposure: For each of the primary elements, H, He, C, O, and Fe, it is necessary to detect at least ten events with energy greater than 10^{15} eV (if the energy spectra of these elements continue unbroken from the spectra that have been measured at lower energies). For H and He this requires at least 1 m^2 sr year. For the heavier elements it requires at least 20 m^2 sr year.

Energy resolution: The energy resolution should be approximately 40% or better. The energy resolution must either be independent of energy or its variation with energy must be well known. Non-Gaussian tails on the high-energy side of the distribution are undesirable and should be minimized.

Charge resolution: It is necessary to be able to resolve boron (Z=5) from carbon (Z=6) when the B/C ratio is as low as 1%, as shown in Figure 7. This requires charge resolution of 0.16 charge units or better, at Z=6. Through Z=26, charge resolution needs to be 0.2 charge units or better. It is also necessary to distinguish cleanly between H and He nuclei incident on the instrument so there is less than a 10% chance of a He nucleus being misidentified as H, or vice versa. (The ability to avoid misidentification of incident H as He depends on separation of incident nuclei from backscattered particles.)

Absolute flux measurement and energy calibration: For comparison with air-shower results, the systematic errors in flux determination must be less than 20%. Since the flux varies so steeply with energy, it is necessary to have systematic errors in energy determination less than 10%.

Cross-calibration: There is no particle accelerator that can reach the highest en-

ergies to be measured by ACCESS; so direct calibration of the calorimeter at these energies is impossible. There are accelerators capable of accelerating elementary particles to the same value of γ as is reached by the TRD. Thus it is essential that ACCESS be configured to measure a significant number of nuclei with $Z \geq 3$ that penetrate both the TRD and calorimeter, so their energy can be measured by both detectors, and the calibration of the two detectors can thus be compared.

3.3.2 Category B

- Measure electron spectrum from 10^{10} eV with sufficient exposure to allow observation of structure at 10^{13} eV.

Particle identification: The flux of cosmic-ray protons is up to 10^4 times as great as that of electrons. Misidentification of an incident proton as an electron is thus a potential source of large error. Consequently, we must require less than one chance in 10^5 of misidentifying a proton as an electron.

Energy resolution: Possible features in the high-energy electron spectrum can be well measured if the energy resolution is $\sigma_E/E = 0.25$ or better. It is important that any changes in energy resolution with energy be understood.

Exposure: An exposure of 2 m^2 sr year will allow identification of possible features in the high-energy electron spectrum.

Absolute energy calibration: 20%

Absolute flux measurement: 20%

- While it would be desirable to have measurements of individual element abundances for all $Z \leq 82$, capability for $Z \leq 40$ would contribute significantly to the third Category B objective. (Note that the rarity of cosmic-ray nuclei with $Z \geq 30$ means that appreciable fluxes will be seen only at energies below a few tens of GeV/nucleon.)

Charge resolution: It is necessary to have well-resolved element peaks at every Z, including odd-Z elements whose abundance may be only 10% of the abundance of adjacent even-Z elements. This requires charge resolution characterized by $\sigma = 0.23$ charge units or better.

Exposure: The exposure required for the measurement of nuclei at least up to Z=60 is similar to that required for the Category A objectives for nuclei of carbon through iron.

4. ACCESS: Baseline Instruments and Payload Support and Interface Module

In order to establish planning for the ACCESS mission, NASA Headquarters identified a baseline set of instruments and requested a formulation study to assess the viability of the mission. A conceptual design of the Payload Support and Interface Module (PSIM), which will support the instruments mechanically, thermally, and electrically during the mission, was included along with the study of the instruments. The final selection and configuration of the instruments will be determined by a competitive Announcement of Opportunity process. Sections 4 and 5 of this document give results of the formulation study, based on the baseline instruments.

This formulation study, and an earlier accommodation study (Wilson & Wefel NASA TP-1999-209202), demonstrate the feasibility of ACCESS as a payload attached to the truss of the International Space Station.

4.1 Payload System Overview

The ACCESS payload consists of the science instruments and the PSIM, which collectively constitute the ACCESS mission flight payload. The baseline science instruments are the calorimeter and the TRD. The TRD instrument contains more than two thousand gas-filled tubes, a gas supply system, and electronics. The TRD determines the velocity of high-energy cosmic-ray particles traversing the instrument. The calorimeter is the heavier of the two science instruments, and it is mounted below the TRD. The calorimeter consists of a carbon target, BGO crystals, and the associated electronics. The calorimeter determines the energy of high-energy particles interacting in the carbon target. These instruments are stacked on top of each other to ensure synergy between their measurements. The stacked configuration provides the framework for the PSIM structural and other supporting subsystems. Both instruments will have charge-identifying capability integrated into their design.

The PSIM functions are similar to those of a spacecraft bus. Its baseline design includes an aluminum truss structure and an electrical interface to the 1553B bus of the ISS external attachment site. The PSIM provides engineering resources, such as power, data, and structural support, to the science instruments by serving as the interface between the science instruments and the ISS external attachment site. The resources supplied by the ISS limit the resources available to the instruments. The ISS resources and the mission operational requirements determine the design criteria for the PSIM. The PSIM design must also be compatible with the Space Shuttle (STS) launch and landing environment, since it serves as the carrier for the science instruments in the Shuttle cargo bay.

4.2 Calorimeter

The calorimeter instrument houses a silicon detector, hodoscope (a trajectory-measuring device), carbon targets, and BGO crystals. The silicon detector, hodoscopes,

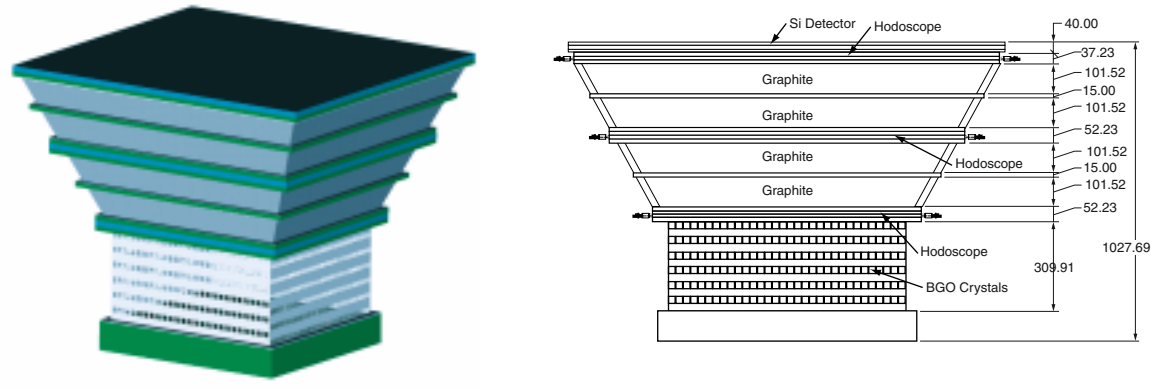

Figure 11. Baseline calorimeter and its cross-sectional view (dimensions are in millimeters)

and the carbon targets make up the upper section of the instrument, and the BGO rods make up the lower section of the instrument. The upper section consists of a segmented silicon matrix, four layers of carbon target, and three hodoscopes. The lower section is comprised of twelve orthogonal layers of BGO rods. The upper section is an inverted frustum of a pyramid with an included aperture angle of 30°. The aperture inlet measures ~1.5 m on a side and at the base measures ~.85 m on a side. The BGO section is a square prism measuring ~.85 m on a side. The full detector has an overall height of ~1 m. Figure 11 shows the baseline calorimeter and its cross-section.

The calorimeter components are supported by a machined aluminum structure with honeycomb panels between the various layers. This structure also provides attachment points for the calorimeter to the PSIM. The baseline calorimeter mass is estimated to be 3200 kg.

4.3 Transition Radiation Detector

The baseline TRD is a layered collection of scintillators, radiators, and detector tubes. The outside dimensions are 3.35 m wide by 1.86 m long and 1.3 m tall. The size of the TRD was chosen to fit into the available volume on the ISS payload external attach site. Figure 12 illustrates the TRD. The baseline TRD mass is estimated to be 930 kg.

Each detection assembly will stack on top of the next, forming the TRD structure that houses tubes and associated electronics. Using this modular approach, it will be possible to test and integrate each assembly individually and verify proper operation. Also, in case of a failure during testing and integration, it will be easy to remove and replace a detection assembly.

The detector tubes of the TRD require a gas management system. It controls the xenon/methane gas supply mixture, the flow of gas from the reservoir to the detector tubes, and the periodic venting of gas on-orbit. The fresh gas mixture from the reservoir fills and replaces old gas in the tubes. Readily available heritage components easily meet the TRD requirements. All of the components (with exception of the tank and possibly the service valves) will be mounted on a common panel with appropriate tube lengths to accommodate this approach. The tank will be mounted under the calorimeter with a final connection to the TRD being made and tested at the PSIM level. The valves are electri-

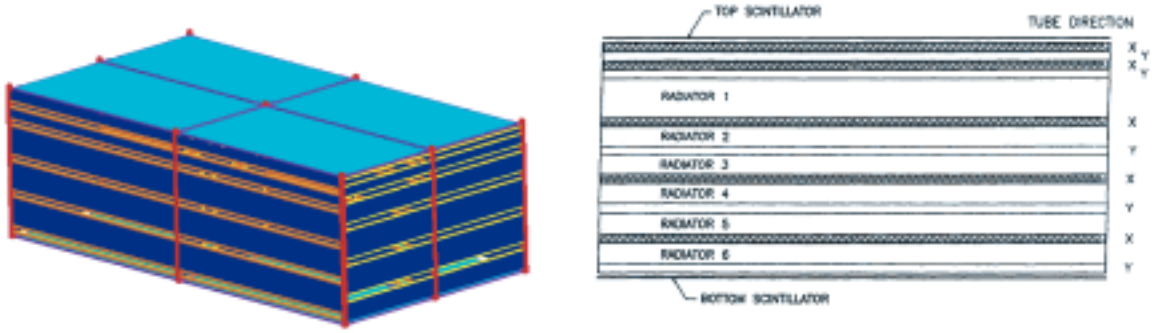

Figure 12. The transition radiation detector (TRD) and its cross-sectional view

cally actuated, and 1 W of continuous power is required for sensors. Additional heater power is required in order to maintain the temperature of the gas management system. Minimal telemetry and commanding is required for monitoring. All of the STS and ISS safety requirements with regard to the gas management system will be implemented.

4.4 Payload Support and Interface Module

The PSIM provides interfaces between the science instruments and the Payload Attach System (PAS) of the ISS. Additionally, it serves as a carrier during launch and landing in the STS cargo bay. The PSIM is designed to house science instruments as well as providing required interfaces so that science measurements can be conducted on-orbit.

The PSIM consists of a mechanical structure, power system, thermal system, command and data handling system, a passive half of the PAS, extravehicular robotics (EVR) grapple fixtures, and extravehicular activity (EVA) handling fixtures. The PSIM design specifications include all of the applicable ISS external payload interface requirements, applicable STS requirements, and ACCESS mission requirements. The PSIM is basically a single string system. However, redundancy will be implemented for mission-critical or safety-critical areas.

4.4.1 Structure

The PSIM is designed to structurally support the ACCESS instruments and components throughout the payload's mission. This requirement includes launch and landing using the Shuttle. It also includes deployment, operations, and retrieval. The baseline PSIM design is shown in Figures 13 and 14.

Structure Description

The PSIM has a truss structure constructed of 7075 aluminum box beams. The main support beams are 15 cm x 15 cm, with a 1 cm wall thickness. Beam cross-section and wall thickness varies in members

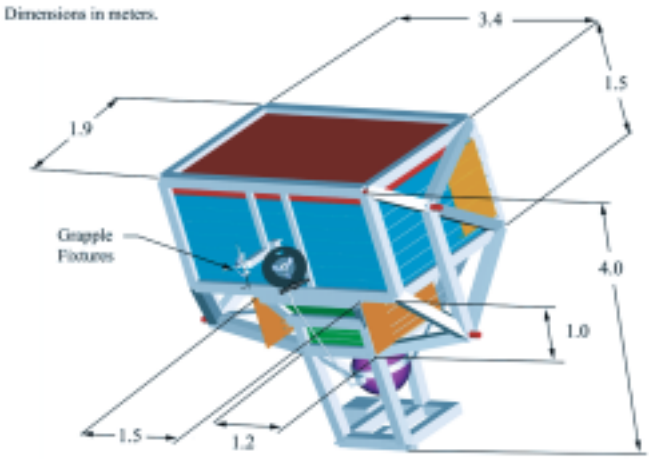

Figure 13. The ACCESS Payload Support and Interface Module, including instruments. The PSIM is the grey framework. (dimensions are in meters)

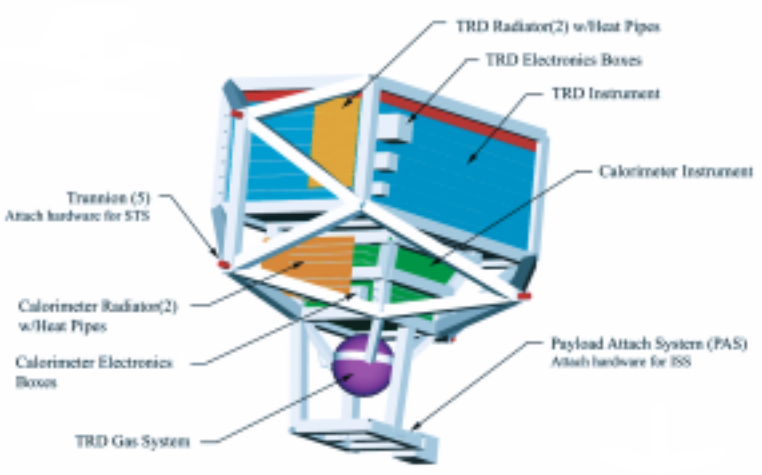

Figure 14. ACCESS payload major components

where loading is not severe. In these members, an optimized combination of smaller cross-section beams and wall thicknesses are used to save weight, while still providing acceptable structural stiffness and load-bearing capability. The ACCESS payload mass is approximately 5500 kg.

Instrument Configuration

The ACCESS instruments attach to the PSIM beams along the edges of each instrument's structure so that the PSIM provides a support frame around each instrument. The PSIM beams then extend from the corners of each framed instrument to the trunnions. The trunnions are attachpoints to the payload bay in the Shuttle.

The instruments are arranged one on top of the other along the central axis of the detectors. The TRD is at the top of the stack, and the calorimeter is at the base of the stack. When the payload is deployed on the ISS, the stack axis is aligned with the ISS zenith axis. This configuration is shown in Figure 15. The configuration of ACCESS installed in the Shuttle cargo bay is shown in Figure 16.

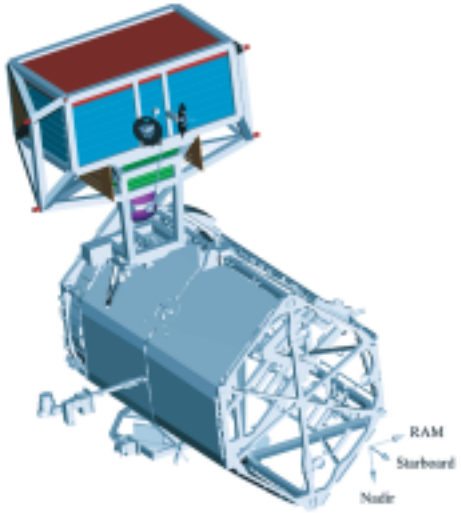

Figure 15. ACCESS ISS configuration

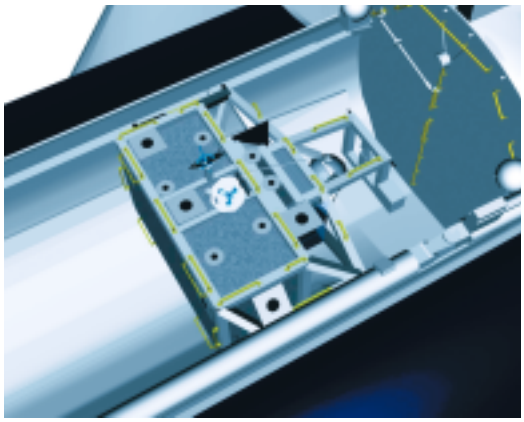

Figure 16. ACCESS in the Shuttle cargo bay

Component Configurations

Instrument components attach to the PSIM structure and also the instrument structures at various points. Instrument electronics boxes mount to the outside of the instrument structure. Radiators are required for heat rejection by both the TRD and the calorimeter. A radiator mounts to both the ram and wake sides of each instrument, for a total of four radiators. Heat pipes run from the radiators around each instrument. The tank of the gas management system required for the TRD mounts to the PSIM below the calorimeter. A gas manifold snakes from the tank, outside the PSIM structure, and to the TRD.

The ACCESS payload attaches to the ISS using the PAS. The system enables a payload to mount mechanically and electrically to the attached payload sites on the ISS. The PAS consists of an active and passive half. The passive half is on the payload side, located below the calorimeter. It consists of three alignment bars and a capture bar for mechanically mating to the ISS, and a universal mating adapter for electrical mating to ISS power and data.

A total of five trunnions secure the ACCESS payload to the Shuttle. Four longeron trunnions attach to the sidewall beams in the Shuttle, and one keel trunnion mounts to the "floor" of the payload bay. Additionally, the ACCESS payload will be connected to the Shuttle Interface Panel (SIP) for power, commands, and telemetry. Two grapple fixtures attach to beams on the +Z side of the PSIM. These fixtures are used as attach points to the STS and ISS robotic arms. The grapples are oriented 90° from one another.

Fields-Of-View

The aperture of the ACCESS payload views space in the zenith direction from its position on the ISS. Since the instruments are in tandem, both instruments point in this direction. Since the TRD has a rectangular aperture, its field-of-view is broader in one plane than the other. The calorimeter has a square aperture and hence a symmetrical field-of-view in two orthogonal planes. The fields-of-view are unobstructed except for the U.S. and Russian solar panels, which rotate through the edges of the field-of-view as they are positioned for optimum solar energy impingement. Preliminary analyses predict that their passage through the ACCESS field-of-view will not be a problem since the panels' low density does not signifi-

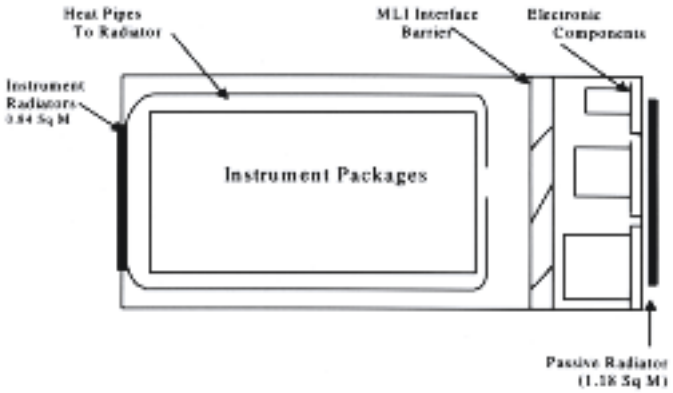

Figure 17. ACCESS thermal design schematic

cantly impede the high-energy particles being captured by the payload aperture. Science data analysis will require knowledge of the ISS solar array configurations that are within the instrument fields-of-view.

4.4.2 Thermal

The thermal design of ACCESS is semi-passive. Heat pipes are used to enhance heat transfer, eliminate hot spots, and help isothermalize the instruments. They provide an optimum heat transfer path to the radiators and minimize their size by lowering the operating temperature.

Heaters are provided for temperature-sensitive components such as the TRD pressure container, and are used to maintain minimum temperature levels in a cold environment during a keep-alive mode. The design is straightforward and, by virtue of the very large time-constant, will provide reliable temperature control with small temperature differences and changes.

The thermal design is based on keep-alive power of 500 W. A design with louvers or a heat pipe could be used if it is determined that the keep-alive power might not be available for extended time periods. Louver efficiency is greatly compromised by the need to include large solar heat loads at the high beta-angles experienced by the ISS. This results in relatively large radiators and will increase cost. Alternatively, loop heat pipes can be combined with passive radiators, since they effectively regulate the condenser area during a cold environment and monitor the heat transfer to space as a function of the source temperature. Their main disadvantage is implementation cost, complexity, and limited space flight heritage.

Conceptual Design

A simplified schematic of the ACCESS thermal design is shown in Figure 17. Heat pipes are used to isothermalize and couple the instruments to the radiators on the wake-facing side of the module, where temperatures are maintained between 0 and 20° C. The attendant stand-alone electronic components are thermally coupled to passive radiators on the ram-facing side, where temperatures are maintained between 0 and 40° C. A multi-layer insulation (MLI) barrier is placed between these two regions to curtail heat transfer when the stand-alone electronics are above 20° C. Both radiators are covered with silver Teflon; all exterior surfaces of the instruments, other than the space radiators, will be covered with MLI.

Heat pipes are mounted in parallel rows and interface with the instruments at locations near the dissipating components, such as the photomultiplier tubes and heat-dissipating detectors and sensors. The aluminum structures afforded by the instruments provide efficient heat transfer paths to the heat pipe evaporators, so that circumferential gradients are minimized. This design also provides efficient heat transfer to space by allowing the radiators to operate at high temperatures - less than 5° C below the average instrument temperature.

Heat pipes are used to isothermalize the instruments by transferring their waste heat directly to the space radiators. The pipes are axially grooved, are 1.25 cm in diameter, and use ammonia as the working substance. It is estimated that 30 heat pipes will be required to service the instruments and radiators. The heat pipes are conventional, constant conductance, and will be embedded in the honeycomb radiator panel on 15 cm centers. (Parallelism between the rows must be maintained to facilitate preflight thermal balance testing.)

Heaters are the thin-wire resistance type, Kapton-insulated, Minco Thermofoil or equivalent. Thermostatic control will be provided for all heaters. Multi-layer insulation will be attached to the outside surfaces of the instruments and PSIM. The blankets consist of 20 sheets of aluminized Kapton with skim-cloth separators.

Radiator areas depend upon orientation, heat generation and the component temperature limits. By isolating the instruments with their relatively narrow temperature range (0 to 20° C) from the associated electronics with their wider temperature range (0 to 40° C), radiator areas and the related cold-case heater power will be minimized. Area calculations were determined from a mathematical model using the SINDA85/ FLUINT program.

Transient Response

The thermal design is greatly simplified by virtue of the large thermal time constant afforded by the 5500 kg mass and an MLI enclosure. Transient response may be defined as a change in temperature, either heating or cooling, caused by a variation in internal heat dissipation or in the external heating environment. The very large thermal time constant inherent in ACCESS may be illustrated by considering a hypothetical cool down in a cold-case environment, when internal power is suddenly reduced to zero. Even with all passive radiators, instrument temperatures are above -10° C at the end of 50 hours. Thus, since ACCESS is very massive and has a large thermal time constant, its internal electronics will remain within a safe temperature range during a temporary power outage.

Pressurized Gas Container

Analysis has been made of the cool down of the pressure vessel containing the xenon and methane gas mixture. The analyses indicate that temperatures do not drop below the allowed minimum in the vessel, even after extended time periods.

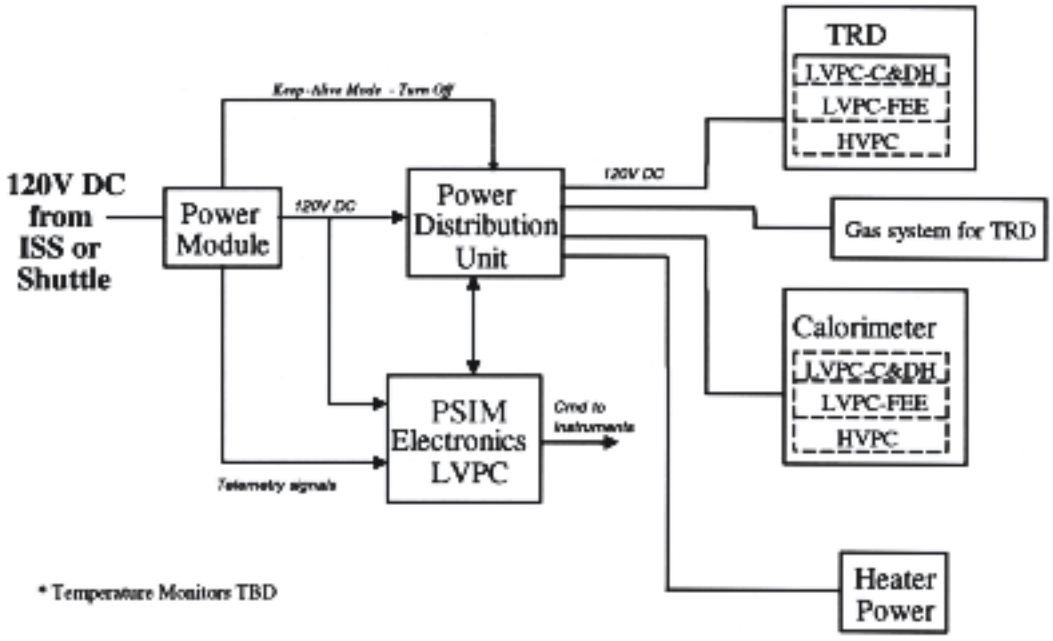

Figure 18. Power system

4.4.3 Power

The power subsystem receives 120 V DC (113 V to 126 V DC) from ISS, via PAS. The baseline power system design is to filter and distribute the 120 V DC to the PSIM subsystems and ACCESS instruments. The users will receive the 120 V DC from the power subsystem, with a total capacity of 710 W available, and make the necessary conversion to the required low voltages and high voltages. Off-the-shelf power converters will be used for conversion to the low voltages. ISS also has a "Keep Alive Mode" where the power allocation to the external payload is limited to 500 W. In this mode, power will only be available to the PSIM electronics, thermal system, and the gas system for the TRD.

The current design for the power subsystem has two main modules: the power module and the power distribution unit (PDU). The power module provides normal mode and common mode filters, inrush current limit, and voltage and current monitors. The PDU provides both switched and unswitched individual power lines to all the users. The PDU provides switched power lines to the PSIM electronics, gas system, and instruments, and unswitched power to the thermal system. The switched power lines will have a solid-state power controller as its switch. All the individual power lines will have over-voltage protection, under-voltage protection, and both voltage and current monitors. The unswitched power will have a fuse in-line for protection. Figure 18 illustrates the ACCESS PSIM power distribution system.

4.4.4 Command and Data Handling

The ACCESS PSIM electronics serve as a bridge between the ACCESS instruments and the ISS power/data interfaces, and manage the operation of the entire payload.

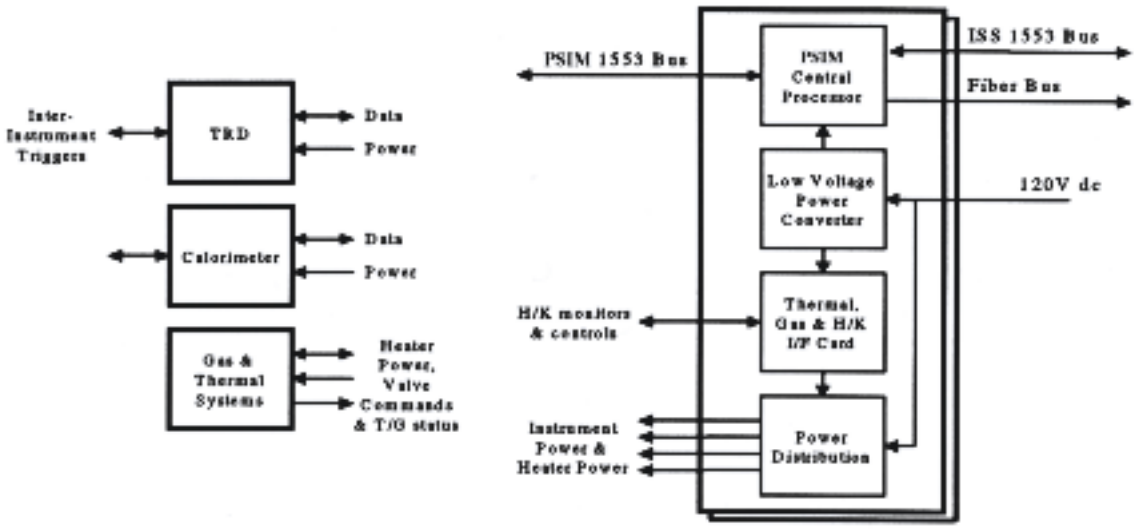

Figure 19. Command and data handling

It is a single integrated unit that distributes commands, collects telemetry, records/stores science and engineering data, performs thermal and gas management housekeeping functions, and switches/distributes instrument power. A block diagram of the system and its interfaces is shown in Figure 19.

A complete redundant unit can be included in the system level design to meet mission level reliability requirements, if necessary. Instrument interfaces consist of only MIL-STD-1553 bus and power, with data exchanged using CCSDS (Consultative Committee for Space Data Systems) packet level protocols. The average combined data rate for all science and engineering data is approximately 300 kbps, and the data system is able to store up to 48 hours of data between dumps. Conditioned, switched, and fused 120 V power is fed to the instruments.

The PSIM electronics support the following modes of operation:

- Shuttle cargo bay: power available, limited functional tests, health/safety monitor
- Shuttle arm: powered OFF
- ISS arm: powered OFF
- ISS site (nominal): full power available, functional tests, normal operations
- ISS site (low power, 500 W): keep-alive power only, health/safety monitors only

The PSIM electronics support the following interfaces and functions:

- ISS 1553 bus: commands and housekeeping data
- ISS fiber bus: science data
- ISS 120 V power: conditioned/ switched/fused service to each instrument
- PSIM 1553 bus: commands, instrument housekeeping, science data
- ACCESS data recorder: 48 hour capacity
- Provides thermal control/monitors (120 V DC heater service)
- Provides gas system control/ monitors
- PSIM electronics is block redundant (cold spare)
- Electronics: 35 W average, local voltage converter
- Power distribution: 15 W average

- Thermal subsystem: 75 W (50 W instruments + 25 W gas system, infrequent)
- Gas subsystem: 100 W peak (200 ms pulse, infrequent)

4.4.5 Extravehicular Robotics and Crew Interfaces

The ACCESS ISS/STS interface design complies with Shuttle and ISS interface requirements including, but not limited to SSP 42131, *Space Station Program Integrated Truss Segments P3 and S3 to Attached Payloads and Unpressurized Cargo Carriers (UCC), Standard Interface Control Document,* and SSP 57003, the *Attached Payload Interface Requirements Document.*

Extravehicular Robotics

The baseline exchange scenario to transfer ACCESS from/to the Shuttle and ISS is by the use of robotics. Specifically, the Shuttle Remote Manipulator System (SRMS) and the Space Station Remote Manipulator System (SSRMS). The scenario requires the use of two grapple fixtures on the payload. The fixtures serve as the interface between the ACCESS payload and the robotic arms.

The location of the grapple fixtures on the payload are in part determined by the geometry and structural constraints of the payload itself, the payload's position in the Shuttle payload bay and on ISS, and the reach of the manipulator. A variety of grapple fixture types are available. As an example, a grapple fixture can be characterized by the payload's need for power and data. ACCESS robotic interfaces will comply with Shuttle and ISS requirements including, but not limited to, *Space Station Program Robotic Systems Integration Standards* (SSP 30550).

To assist the crewmembers in grappling and docking ACCESS, a visual system of cameras and targets will be used as necessary. In addition, all transport activities can be monitored by an array of cameras on the Shuttle and ISS.

Extravehicular Activity

ACCESS mission operations will implement EVA or intra-vehicular activity (IVA) on contingency cases only. ACCESS EVA and IVA interfaces will comply with Shuttle and ISS requirements including, but not limited to, those described in *Extravehicular Activity (EVA) Standard Interface Control Document* (SSP 30256) and *ISS Flight Crew Integration Standard* (SSP 50005, NASA-STD-3000/T).

ACCESS will have the appropriate EVA corridors necessary for contingency EVA accessibility. According to the *ISS Truss to Attached Payload and UCC Interface Control Document* (SSP 42131), access is necessary to support removal and/or disassembly of the PAS Orbital Replacement Units. This requirement is also in accordance with SSP 30256 and SSP 50005.

ACCESS will also be equipped with an EVA releasable capture bar to assist in contingency manipulation of the payload in case of PAS malfunction.

Other Crew Interfaces

Prior to Space Shuttle-to-ISS transfer, "health and housekeeping" of ACCESS will be monitored by IVA crewmembers and ACCESS ground support. A visual

checkout of the payload will also be performed by the crew directly from the aft flight deck (if they have a clear field-of-view) and using payload bay and SRMS cameras. Additionally, ACCESS will be periodically monitored (health, housekeeping, etc.) by the ISS crew.

5. Mission Plan

5.1 Mission Description

ACCESS is a large-area detector system designed for a four-year exposure to space. The detector system is a complement of cosmic-ray science instruments designed to investigate the origin, acceleration, and propagation of high-energy cosmic rays.

It is designed and configured to occupy one of the zenith-pointing full truss sites on the ISS. ACCESS science data requires pointing knowledge of the instruments. The ISS pointing knowledge accuracy of 2 to 3 degrees for truss sites is within the ACCESS science allowables. The STS will launch the mission from the Kennedy Space Center in Florida. Once the Shuttle reaches the orbit and docks on the ISS, ACCESS will be taken out of the cargo bay with the SRMS and it will be handed to the SSRMS. The SSRMS will transfer the payload to the site, and it will be mated with the ISS PAS on the external site. The mission will be initiated with the In-Orbit-Checkout (IOC), and normal mission operation will begin once the IOC is complete and there are no anomalies.

The duration of the mission on ISS is four years with an 80% operating cycle, and it has no planned human intervention. Hence, both safety and reliability are key factors in all mission planning. Finally, at the end of the mission, ACCESS will be retrieved from its ISS berth and returned to Earth, again with safety being a paramount goal.

5.2 Mission Requirements Flow-down

A summary of the flow-down of the primary instrument requirements is given in Figure 20. The ACCESS science questions drive the flow-down of requirements into the measurement capabilities. These include resolution of charge and energy, energy spectra range, and spatial and temporal exposure. Ultimately, these drive the engineering requirements of accommodating instruments with the size and mass needed to complete the science mission.

Figure 20. ACCESS traceability matrix

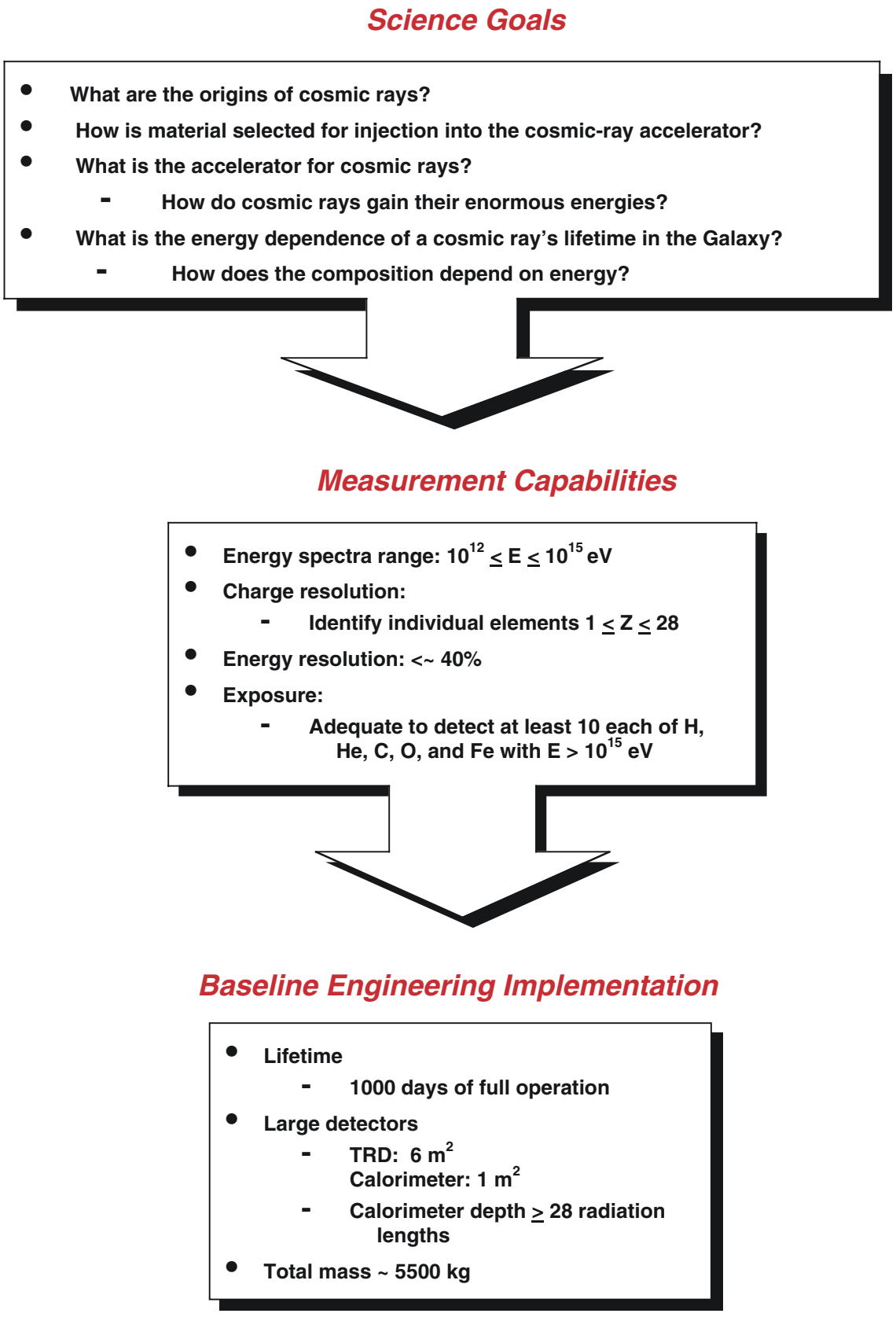

5.3 Mission Timeline

5.3.1 STS Launch and ISS Docking

After a routine Shuttle launch, rendezvous, and docking with the ISS, ACCESS is prepared for transfer from the Shuttle cargo bay to its position on the ISS truss. This is accomplished by a handoff of ACCESS between robotic arms and fixtures described earlier in Section 4.4.5.

An example of the robotic installation timeline and choreography is described in Table 1, and shown in Figures 21a-d.

Action	**Duration (minutes)**	**Cumulative duration, in min.**
The Space Station Remote Manipulator System (SSRMS) releases one Mobile Remote Servicer Base System (MBS) Power Data Grapple Fixture (PDGF) and uses the appropriate MBS PDGF as its operating base for the payload.	15	
The SSRMS is positioned in the payload handoff zone.	15	30 (0.5 hr)
The payload is grappled by the Shuttle Remote Manipulator System (SRMS).	15	45 (0.75 hr)
The payload is unberthed by the SRMS.	30	75 (1.25 hr)
The SRMS positions the payload for handoff to the SSRMS.	15	90 (1.5 hr)
Once the payload is in position, the SSRMS maneuvers and grapples the second payload Flight Releasable Grapple Fixture (FRGF). The SSRMS is at Mobile Transport (MT) position S1 Bay 6.	15	105 (1.75 hr)
Once a good SSRMS grapple is confirmed, the SRMS releases the payload and maneuvers to a clear position.	10	115 (1 hr 55 min)
The SSRMS maneuvers the payload into a preinstallation position.	30	145 (2.5 hr)
The SSRMS positions the payload into the capture envelope. The MT does not need to be translated during this operation.	30	175 (3 hr)
Once a good payload interface is confirmed, the SSRMS releases the payload and reconfigures.		

Table 1. EVR installation timeline

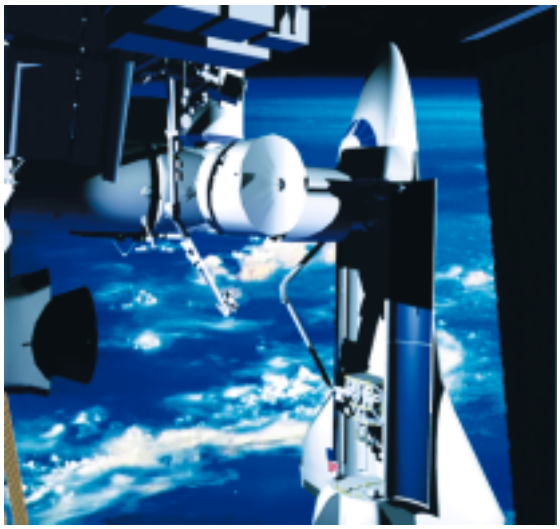

Figure 21a. ACCESS on SRMS

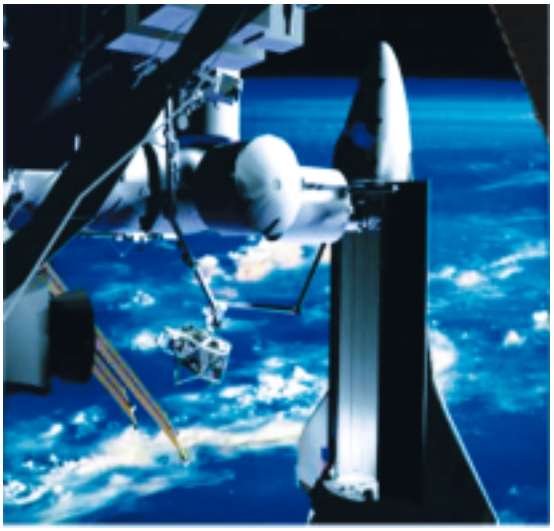

Figure 21b. ACCESS hand-over to SSRMS

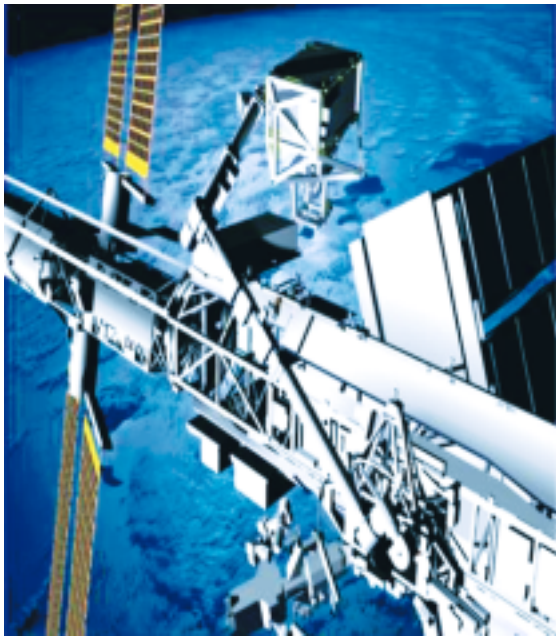

Figure 21c. ACCESS on SSRMS

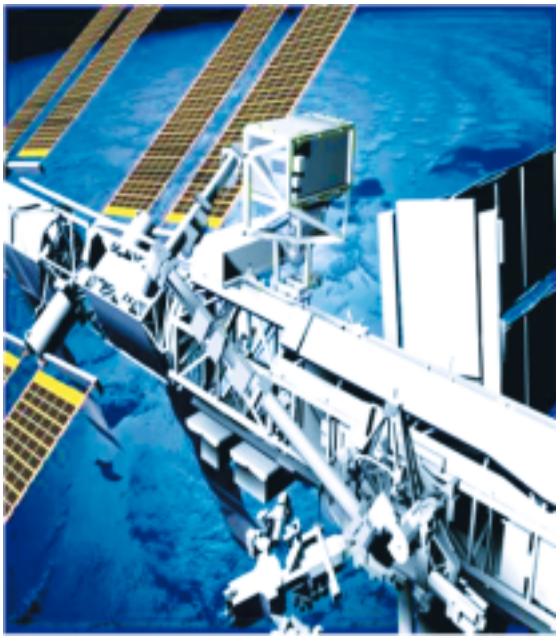

Figure 21d. ACCESS on ISS S3 in-board upper truss

5.3.2 Instrument Activation and Major Scheduled Events

The ACCESS payload will be activated shortly after its installation onto the ISS inboard upper truss. There currently are no major scheduled events planned beyond normal data taking by the TRD and calorimeter. However, the baseline TRD will require periodic replenishing of xenon-methane gas to compensate for nominal leakage of gas.

5.3.3 De-activation and Retrieval

No special de-activation procedures have been identified for the instruments except for power-down. Retrieval of ACCESS will follow a reversal of the steps and timeline shown in Table 1.

5.4 Mission Operations Concept (Including Ground Operations)

The ACCESS mission operations are enabled by simple and routine instrument operations. The moderate data rate allows the use of existing capabilities of the MSFC-designed Telescience Resource Kit (TReK). The TReK is ISS-sponsored and supported for ISS payloads. It is low-cost and low-risk for implementation.

The normal ACCESS mission operations are very routine. ACCESS will generate data and send it to the ground, either in real time or as playback data. The science data will be distributed to the instrument teams for processing, and the health and safety data will be processed to identify any problems with the instruments or the PSIM. ACCESS operations may be affected by the South Atlantic Anomaly (SAA). If so, stored commands will be used to adjust the configuration of the instrument during SAA excursion. ACCESS will have a background counter that will be used as a backup to the stored commands. Periodically, the gas in the baselined TRD instrument will be replenished.

The instrument operations will be scheduled with other ISS users. ACCESS may be scheduled to be in a low power mode up to 20% of the time to accommodate high power demand from other ISS activities. Real-time contact with the ground will also be scheduled. Between contacts, ACCESS will store the data. During the contact, ACCESS will send both the real-time data and the stored data. The combined data rate should be on the order of 0.5 Mbps. The real-time and playback instrument data will be combined and time-ordered on the ground prior to distributing it to the instrument teams for science processing.

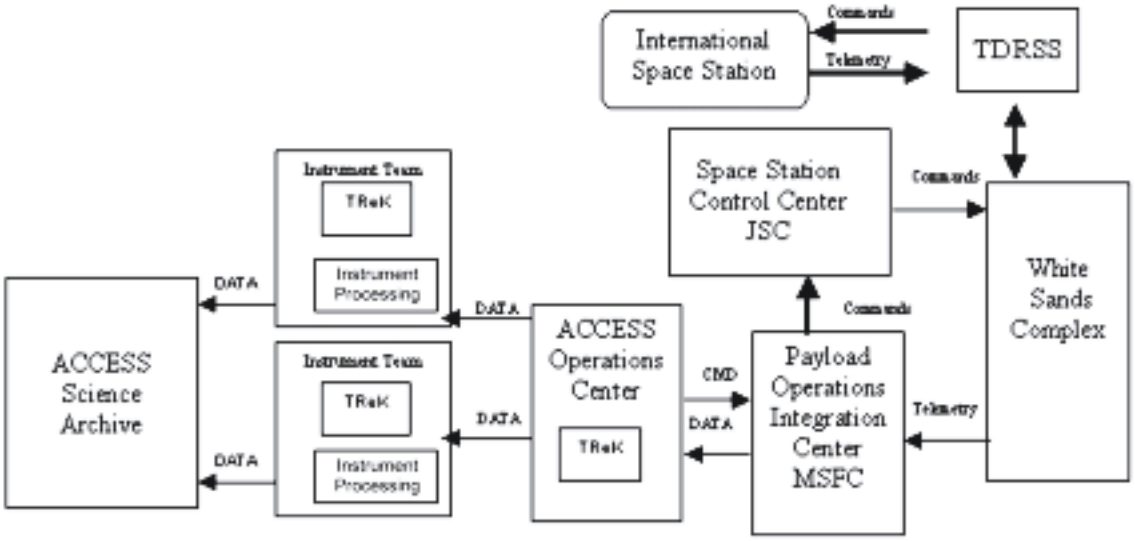

Figure 22. ACCESS ground system

Figure 22 shows the ground system. The Payload Operations Integration Center (POIC) at MSFC is responsible for coordinating ISS payload operations. ACCESS will be operated from the ACCESS Operations Center. This Center will use the TReK to process health and safety data, to receive science data, and to send commands. The TReK system also provides access to ISS audio and video. The time-ordered science data will be distributed to the instrument teams for processing. After processing by the instrument teams, the science data will be sent to the archive for storage and distribution. The instrument teams can also use TReK workstations to monitor the status of the operations; however, commanding is restricted to the system in the ACCESS operations center.

The ACCESS operations center will be largely automated for normal operations. During normal business hours, the staff will evaluate the performance of the PSIM and verify that the data is being delivered. When the operations center is not staffed, autonomous systems will monitor the health and safety of ACCESS and the data flows, and alert an on-call staff member if a problem occurs.

The operations center will be staffed around the clock during launch, installation, and initial instrument checkout. In addition, some of the ACCESS team will be co-located at the POIC at MSFC to coordinate the ACCESS operations with the rest of the Space Station and Shuttle team. Similar co-location will occur when ACCESS is removed from the Space Station and returned to earth.

5.5 Mission Data Products

The ACCESS mission intends to archive all data at the National Space Science Data Center (NSSDC). The NSSDC archive will be stored in an approved standard format. This archive will, at first, consist of Level 0 raw data and Level 1 processed data. Level 2 data consisting of energy spectra for the abundant elements up through iron will eventually be archived as well. However, in order to accumulate statistics and validate the spectra, this will probably not be available until the end of the mission. It may be possible to release energy spectra for the more abundant elements at low energies on a shorter timescale.

References

Aglietta, M., et al. 1994, Phys. Lett. B, **337**, 376
Aglietta, M., et al. 1998, Astropart. Phys, **9**, 185
Allen, S., et al. 1997, ApJ, **L97**, 487
Ambrosio, M., et al. 1992, Phys. Rev. D, **46**, 895
Ambrosio, M., et al. 1997, Phys. Rev. D, **56**, 1418
Apanasenko, A.V., et al. 1999, 26th ICRC, **3**, 163
Asakimori, K., et al. 1998, ApJ, **502**, 278
Bahcall, J., & Waxman, E. 1999, LANL preprint (hep-ph/9902383)
Bakatanov, V.N., et al. 1999, Astropart. Phys, **12**, 19
Binns, W., et al. 1988, ApJ, **324**, 1106
Bird, D.J., et al. 1993, Phys. Rev. Lett, **71**, 3401
Chevalier, R.A. 1983, ApJ, **272**, 765
Dorfi, E.A., & Bohringer, H. 1993, A&A, **273**, 251
Engelmann, J.J., et al. 1990, A&A, **233**, 96
Engler, J., et al. 1999, 26th ICRC, **1**, 349
Greisen, K. 1966, Phys. Rev. Lett, **16**, 748
Grigorov, N.L., et al. 1971, 12th ICRC, **5**, 1746
Hillas, A.M. 1984, Ann. Rev. of A&A, **22**, 425
Inoue, N., et al. 1999, 26th ICRC, 1, 357
Juliusson, E., et al. 1972, Phys. Rev. Lett, **29**, 445
Kobayashi, T., et al. 1999, 26th ICRC, **3**, 61
Meyer, J.P. 1985, 19th ICRC, **9**, 141
Meyer, J.P., et al. 1997, ApJ, **487**, 182
Müller, D., et al. 1991, ApJ, **374**, 356
NASA Office of Space Science. 1999. Cosmic Journeys — To the Edge of Gravity, Space, and Time - Structure and Evolution of the Universe Roadmap: 2003-2023.
NRC, Astronomy and Astrophysics Survey Committee. 2000. Astronomy and Astrophysics in the New Millennium
NRC, Committee on Cosmic-ray Physics. 1995. Opportunities in Cosmic-Ray Physics and Astrophysics
NRC, Committee on Solar and Space Physics. 1995. A Science Strategy for Space Physics
Nishimura, J., et al. 1980, ApJ, **238**, 394
Nishimura, J., et al. 1997, 25th ICRC, **4**, 223
Ptuskin, V., & Ormes, J. 1995, 24th ICRC, **3**, 56
Seckel, D., et al. 1999, 26th ICRC, **3**, 171
Seo, E.S., & Ptuskin, V. 1994, ApJ, **431**, 705
Smith, L.H., et al. 1973, ApJ, **180**, 987
Swordy, S.P., et al. 1990, ApJ, **349**, 625
Takahashi, Y. 1998, Nucl. Phys. B, **60B**, 83
Takeda, M., et al. 1998, Phys. Rev. Lett, **81**, 1163
Waxman, E., & Bahcall, J. 1998, Phys. Rev. D, **59**, 023002
Wilson, T., & Wefel, J. (ed.) 1999, ACCESS Accommodation Study Report, NASA TP-1999-209202
Zatsepin, G.T., & Kuz'min, V.A. 1966, JETP Lett, **4**, 78

Acronyms

ACCESS - Advanced Cosmic-ray Composition Experiment for the Space Station
AGASA - Akeno Giant Air Shower Array
AGN - Active galactic nuclei
ATIC - Advanced Thin Ionization Calorimeter
BACH - Balloon Air CHerenkov experiment
B/C ratio - boron/carbon ratio
BGO - Bismuth germanate
C&DH - Command and data handling
CCSDS - Consultative Committee for Space Data Systems
CMD - Command
CRN - Cosmic-Ray Nuclei experiment
CRS - Cosmic-ray source
DICE - Dual Imaging Cherenkov Experiment
E - Energy
EAS-TOP - Extensive Air Shower - TOP detector above the Gran Sasso
EUSO - Extreme Universe Space Observatory
EVA - Extravehicular activity
EVR - Extravehicular robotics
FEE - Front-end electronics
FIP - First ionization potential
FRGF - Flight Releasable Grapple Fixture
GSFC - NASA Goddard Space Flight Center
HEAO - High-Energy Astrophysics Observatory
HEGRA - High-Energy Gamma Ray Astronomy experiment
H/K - Housekeeping
HVPC - High-voltage power converter
ICRC - International Cosmic Ray Conference
I/F - Interface
IOC - In-Orbit-Checkout
ISS - International Space Station
IVA - Intra-vehicular activity
JACEE - Japanese-American Cooperative Emulsion Experiment
JSC - NASA Johnson Space Center
KASCADE - KArlsruhe Shower Core and Array DEtector
LVD - Large Volume Detector in the Gran Sasso
LVPC - Low-voltage power converter
MACRO - Monopole, Astrophysics, and Cosmic Ray Observatory
MBS - Mobile Remote Servicer Base System
MLI - Multi-layer insulation
MSFC - NASA Marshall Space Flight Center
MSU - Moscow State University
MT - Mobile Transport
MWPC - Multi-wire proportional counter
NSSDC - National Space Science Data Center
OSS - NASA's Office of Space Science
OWL - Orbiting Wide-angle Light collectors

PAS - Payload Attach System
PDGF - Power Data Grapple Fixture
PDU - Power distribution unit
POIC - Payload Operations Integration Center
PSIM - Payload support and interface module
RUNJOB - Russian Nippon Joint Balloon experiment
SAA - South Atlantic Anomaly
SEU - NASA's OSS Structure and Evolution of the Universe theme
SIP - Shuttle Interface Panel
SNR - Supernova remnant
SRMS - Shuttle Remote Manipulator System
SS - Solar system
SSRMS - Space Station Remote Manipulator System
STS - Space Shuttle (Space Transportation System)
TDRSS - Tracking and Data Relay Satellite System
T/G - thermal/gas subsystems
TR - Transition radiation
TRACER - Transition Radiation Array for Cosmic Energetic Radiation
TRD - Transition radiation detector
TReK - Telescience Resource Kit
Z - Nuclear charge/atomic number

NP-2000-05-056-GSFC